Weak turbulence theory and simulation of the gyro-water-bag model

Nicolas Besse,* Pierre Bertrand,† Pierre Morel,‡ and Etienne Gravier§
Laboratoire de Physique des Milieux Ionisés et Applications, UMR CNRS 7040, Faculté de Sciences et Techniques, Université Henri Poincaré, Bd des Aiguillettes, B.P. 239, 54506 Vandoeuvre-lès-Nancy Cedex, France
(Received 26 October 2007; published 30 May 2008)

The thermal confinement time of a magnetized fusion plasma is essentially determined by turbulent heat conduction across the equilibrium magnetic field. To achieve the study of turbulent thermal diffusivities, Vlasov gyrokinetic description of the magnetically confined plasmas is now commonly adopted, and offers the advantage over fluid models (MHD, gyrofluid) to take into account nonlinear resonant wave-particle interactions which may impact significantly the predicted turbulent transport. Nevertheless kinetic codes require a huge amount of computer resources and this constitutes the main drawback of this approach. A unifying approach is to consider the water-bag representation of the statistical distribution function because it allows us to keep the underlying kinetic features of the problem, while reducing the Vlasov kinetic model into a set of hydrodynamic equations, resulting in a numerical cost comparable to that needed for solving multifluid models. The present paper addresses the gyro-water-bag model derived as a water-bag-like weak solution of the Vlasov gyrokinetic models. We propose a quasilinear analysis of this model to retrieve transport coefficients allowing us to estimate turbulent thermal diffusivities without computing the full fluctuations. We next derive another self-consistent quasilinear model, suitable for numerical simulation, that we approximate by means of discontinuous Galerkin methods.

DOI: 10.1103/PhysRevE.77.056410 PACS number(s): 52.35.Ra, 52.65.−y, 52.30.−q

I. INTRODUCTION

The energy confinement time in controlled fusion devices is governed by the turbulent evolution of low-frequency electromagnetic fluctuations of nonuniform magnetized plasmas. Microinstabilities are now commonly held responsible for this turbulence transport giving rise to anomalous radial energy transport in tokamak plasmas. Low-frequency ion-temperature-gradient-driven (ITG) instability is one of the most serious candidates to account for the anomalous transport [1], as well as the so-called trapped electron modes [2]. The computation of turbulent thermal diffusivities in fusion plasmas is of prime importance since the energy confinement time is determined by these transport coefficients. During recent years, ion turbulence in tokamaks has been intensively studied both with fluid (see, for instance, [3–5]) and gyrokinetic simulations using PIC codes [6–8] or Vlasov codes [9–12].

It is now well known that the level of description, namely kinetic or fluid, may significantly impact the instability threshold as well as the predicted turbulent transport. Consequently, it is important that gyrokinetic simulations quantify the departure of the local distribution function from a Maxwellian, which constitutes the usual assumption of fluid closures.

In a recent paper [13] a comparison between fluid and kinetic approach has been addressed by studying a three-dimensional kinetic interchange. A simple drift kinetic model is described by a distribution depending only on two spatial dimensions and parametrized by the energy. In that case it appears that the distribution function is far from a Maxwellian and cannot be described by a small number of moments. Wave-particle resonant processes certainly play an important role and most of the closures that have been developed will be inefficient.

On the other hand, although more accurate, the kinetic calculation of turbulent transport is much more demanding in computer resources than fluid simulations. This motivated us to revisit an alternative approach based on the water-bag representation.

Introduced initially by DePackh [14], Feix and coworkers [15–17], the water-bag model was shown to bring the bridge between fluid and kinetic description of a collisionless plasma, allowing to keep the kinetic aspect of the problem with the same complexity as the fluid model. Furthermore this model was extended into a double water-bag by Berk and Roberts [18] and Finzi [19], and generalized to the multiple water-bag [20–23].

The aim of this paper is to use the water-bag description for gyrokinetic modeling. Let us notice that the water-bag-like weak solution of the gyrokinetic equation has the advantage of avoiding the treatment of singularities in the complex plane, encountered in the Landau description of Vlasovian plasmas, by introducing Landau contours and analytic continuation of the quantities involved.

After a brief introduction of the well-known gyrokinetic equations hierarchy, we present the gyro-water-bag (GWB) model. Then we perform a quasilinear analysis of the GWB system allowing us to show that the model possesses some invariants such as the total density, momentum, and energy. Next we derive quasilinear equations for describing weak turbulence of magnetized plasma in a cylinder, in a form which is well suited for computation. Therefore, we propose

*Also at Institut de Mathématiques Elie Cartan UMR CNRS 7502, Faculté de Sciences et Techniques, Université Henri Poincaré, Bd des Aiguillettes, B.P. 239, 54506 Vandoeuvre-lès-Nancy Cedex, France; besse@iecn.u-nancy.fr; nicolas.besse@lpmi.uhp-nancy.fr
†pierre.bertrand@lpmi.uhp-nancy.fr
‡pierre.morel@lpmi.uhp-nancy.fr
§etienne.gravier@lpmi.uhp-nancy.fr

a numerical approximation scheme, based on discontinuous Galerkin methods to solve these equations. Then we present some numerical results obtained in the context of plasma turbulence driven by ITG instabilities. Finally we compare with results given by fully nonlinear simulations.

II. GYRO-WATER-BAG MODEL

A. Gyrokinetic equation

Strictly speaking, one must solve a six-dimensional kinetic equation to determine the statistical distribution function of one particle. However, for strongly magnetized plasmas nonlinear gyrokinetic equations are traditionally derived through a multiple space-time scale expansion that relies on the existence of one or more small dimensionless ordering parameters. For instance, the Larmor radius ρ is much smaller than the characteristic background magnetic field or plasma density and temperature nonuniformity length scale L. Besides the cyclotron motion is faster than the turbulent motion at least during the early phase of the nonlinear interactions. The conventional procedure [24], to derive the gyrokinetic Vlasov equations consists in computing an iterative solution of the gyroangle-averaged Vlasov equation perturbatively expanded in powers of the dimensionless parameter ρ/L. A modern foundation of nonlinear gyrokinetic theory [25–27] is based on a two-step Lie-transform procedure, from particle Hamiltonian dynamics to gyrocenter motion through guiding-center dynamics and a reduced variational principle [27,28], allowing us to derive self-consistent expressions for the nonlinear gyrokinetic Vlasov Maxwell equations. Therefore, for strongly magnetized plasmas, nonlinear gyrokinetic theory allows us to recast the Vlasov equation into a five-dimensional equation in which the fast gyroangle does not appear explicitly but in which the main particle information is not lost.

Let $f=f(t,\mathbf{r},v_\parallel,\mu)$ be the gyrocenter distribution function for ions. Therefore, the nonlinear gyrokinetic equations as derived in [24–27] are

$$D_t f = \partial_t f + \dot{X}_\perp \cdot \nabla_\perp f + \dot{X}_\parallel \cdot \nabla_\parallel f + \dot{v}_\parallel \partial_{v_\parallel} f = 0 \tag{1}$$

with

$$\dot{X}_\parallel = v_\parallel \mathbf{b}, \quad \dot{X}_\perp = v_\mathbf{E} + v_{\nabla B} + v_c,$$

$$v_\mathbf{E} = \frac{1}{B_\parallel^*}\mathbf{b} \times \nabla \mathcal{J}_\mu \phi,$$

$$v_{\nabla B} = \frac{\mu}{q_i B_\parallel^*}\mathbf{b} \times \nabla B,$$

$$v_c = \frac{m_i v_\parallel^2}{q_i B_\parallel^*}\left(\frac{\mathbf{b} \times \nabla B}{B} + \frac{(\nabla \times \mathbf{B})_\perp}{B}\right) = \frac{m_i v_\parallel^2}{q_i B_\parallel^*}\mathbf{b} \times \frac{\mathbf{N}}{R_c},$$

$$\dot{v}_\parallel = -\frac{1}{m_i}\left(\mathbf{b} + \frac{m_i v_\parallel}{q_i B_\parallel^*}\mathbf{b} \times \frac{\mathbf{N}}{R_c}\right) \cdot (\mu \nabla B + q_i \nabla \mathcal{J}_\mu \phi),$$

$$\mathbf{B}^* = \mathbf{B} + \frac{m_i v_\parallel}{q_i} \nabla \times \mathbf{b}, \quad B_\parallel^* = \mathbf{B}^* \cdot \mathbf{b},$$

where $\mathbf{b}=\mathbf{B}/B$ denotes the unit vector along magnetic field line, $\mathcal{J}_\mu$ denotes the gyroaverage operator, $\mathbf{N}/R_c$ is the field line curvature, $q_i=Z_i e$, $e>0$ being the elementary Coulomb charge, and $\mu=m_i v_\perp^2/(2B)$ is the first adiabatic invariant of the ion gyrocenter. The structure of the distribution function f, solution of (1), is of the form

$$f(t,\mathbf{r},v_\parallel,\mu) = \sum_\ell f_\ell(t,\mathbf{r},v_\parallel)\delta(\mu-\mu_\ell). \tag{2}$$

Let us notice that an interesting problem is to know what is the asymptotic statistical distribution function in μ in (2) if we consider an infinite number of magnetic moments, because it allows us to save CPU time and memory space in numerical codes. In [29–31], the authors take the distribution $m_i \exp(-\mu B/T_{i0})/T_{i0}$. If we now suppose $k_\perp \rho_i$ small and neglecting all terms smaller than $O(k_\perp^2 \rho_i^2)$, then we obtain the Poisson equation

$$-Z_i q_i \nabla_\perp \cdot \left(\frac{n_i \rho_i^2}{T_i}\nabla_\perp \phi\right) = \lambda_{D_i}^2 Z_i q_i \frac{n_{i0}}{T_{i0}}\Delta\phi + Z_i \int 2\pi \frac{\Omega_i}{q_i} d\mu dv_\parallel \mathcal{J}_\mu f - n_e, \tag{3}$$

where $\rho_i^2=v_{thi}^2/\Omega_i^2=T_i/(m_i\Omega_i^2)$ is the ion Larmor radius, and $\lambda_{D_i}^2=k_B T_i/(4\pi\varepsilon_0 Z_i^2 e^2 n_{i0})$ is the ion Debye length. The left-hand side of Eq. (3) corresponds to the difference between the gyroaveraged density $\frac{\Omega_i}{q_i}\int d\mu dv_\parallel \mathcal{J}_\mu f$ and the laboratory ion density N_i which is the lowest contribution to the density fluctuations provided by the polarization drift.

Since we are mainly interested in this paper by the kinetic-vs-fluid problem, the first equation to be addressed is to look at the effects of the transverse drift-velocity $\mathbf{E}\times\mathbf{B}$ coupled to the parallel dynamics while the curvature effects are considered as a next stage of the study and are consequently beyond the scope of the present paper. As a result, in a sequel we deal with a reduced drift kinetic model in cylindrical geometry by making the following approximations.

(i) In addition of cylindrical geometry, we suppose that the magnetic field $\mathbf{B}$ is uniform and constant along the axis of the column (z coordinate, $\mathbf{B}=B\mathbf{b}=B\mathbf{e}_z$). It follows that the perpendicular drift velocity does not admit any magnetic curvature or gradient effect and especially we have $\mathbf{B}^*=\mathbf{B}$. It is important to point out that the water-bag concept (i.e., phase space conservation), that will be presented below, is not affected by adding finite Larmor radius or curvature terms, except, of course, a more complicated algebra.

(ii) We suppose a finite discrete sequence of adiabatic invariants $\Xi=\{\mu\}$ linked to a finite discrete sequence of ion Larmor radius $\Lambda=\{\rho\}$ by $\mu=\rho^2\Omega_i q_i/2$. The linear differential operator of gyroaveraging $\mathcal{J}_\mu$ becomes the Bessel function $J_0(k_\perp\sqrt{2\mu}/\sqrt{\Omega_i q_i})$ in the Fourier space.

(iii) We linearize the expression for the polarization density, n_{pol}, in Eq. (3),

$$n_{\mathrm{pol}} = \nabla_\perp \cdot \left(\frac{n_i}{B\Omega_{ci}} \nabla_\perp \phi \right),$$

by approximating n_i to the background density of the Maxwellian distribution function n_{i0}, and by assuming that the ion cyclotron frequency Ω_i is a constant Ω_0. Moreover, we assume that the ion Debye length λ_{D_i} is small compared to the ion Larmor radius ρ_i.

(iv) The electron inertia is ignored, i.e., we choose an adiabatic response to the low-frequency fluctuations for the electrons. In other words, the electrons density follows the Boltzmann distribution

$$n_e = n_{e0} \exp\left(\frac{e}{k_B T_e} (\phi - \lambda \langle \phi \rangle_{\mathcal{M}}) \right),$$

where $\langle \phi \rangle_{\mathcal{M}}$ denotes the average of the electrical potential ϕ over a magnetic surface. The parameter λ is a control parameter for zonal flows. It takes the value zero or one.

Under theses assumptions the evolution of the ion gyrocenter distribution function $f_\mu = f_\mu(t, \mathbf{r}_\perp, z, v_\parallel)$ obeys the gyrokinetic Vlasov equation

$$\partial_t f_\mu + \mathcal{J}_\mu \mathbf{v}_{\mathbf{E}} \cdot \nabla_\perp f_\mu + v_\parallel \partial_z f_\mu + \frac{q_i}{m_i} \mathcal{J}_\mu E_\parallel \partial_{v_\parallel} f_\mu = 0 \qquad (4)$$

for the ions (q_i, M_i), coupled to an adiabatic electron response via the quasineutrality assumption

$$-\nabla_\perp \cdot \left(\frac{n_{i0}}{B\Omega_0} \nabla_\perp \phi \right) + \frac{e\tau n_{i0}}{T_{i0}} (\phi - \lambda \langle \phi \rangle_{\mathcal{M}}) = 2\pi \sum_{\mu \in \Xi} \int_{\mathbb{R}} \frac{\Omega_i}{q_i} \mathcal{J}_\mu f_\mu(t, \mathbf{r}, v_\parallel) dv_\parallel - n_{i0}. \qquad (5)$$

Here $q_i = Z_i e$, $Z_i n_{i0} = n_{e0}$, $T_e = T_{e0}$, $\tau = T_{i0}/T_{e0}$, $\lambda \in \{0,1\}$, $\mathbf{E} = -\nabla\phi$, and $\mathbf{v}_E$ is the $\mathbf{E} \times \mathbf{B}/B^2$ drift velocity. The ion temperature profile T_{i0} and the ion density profile n_{i0} vary along the radial direction.

The most important and interesting feature is that f depends, through a differential operator, only on the velocity component $v_\parallel$ parallel to $\mathbf{B}$.

B. GWB model

Let us now turn back to the gyrokinetic equation (4). Since the distribution $f_\mu(t, \mathbf{r}_\perp, z, v_\parallel)$ takes into account only one velocity component $v_\parallel$ a water-bag solution can be considered [21]. Let us consider $2\mathcal{N}$ nonclosed contours in the $(\mathbf{r}, v_\parallel)$-phase space (see Fig. 1) labeled $v^+_{\mu j}$ and $v^-_{\mu j}$ (where $j = 1, \ldots, \mathcal{N}$, $\mu \in \Xi$) such that $\cdots < v^-_{\mu j+1} < v^-_{\mu j} < \cdots < 0 < \cdots < v^+_{\mu j} < v^+_{\mu j+1} < \cdots$ and some real numbers $\{\mathcal{A}_{\mu j}\}_{j \in [1,\mathcal{N}], \mu \in \Xi}$ that we call bag heights (see Fig. 2). We then define $f_\mu(t, \mathbf{r}_\perp, z, v_\parallel)$ as

$$f_\mu(\mathbf{t}, \mathbf{r}_\perp, z, v_\parallel) = \sum_{j=1}^{\mathcal{N}} \mathcal{A}_{\mu j} \{ \mathcal{H}[v_\parallel - v^-_{\mu j}(t, \mathbf{r}_\perp, z)] - \mathcal{H}[v_\parallel - v^+_{\mu j}(t, \mathbf{r}_\perp, z)] \}, \qquad (6)$$

where $\mathcal{H}$ is the Heaviside unit step function. The function (6)

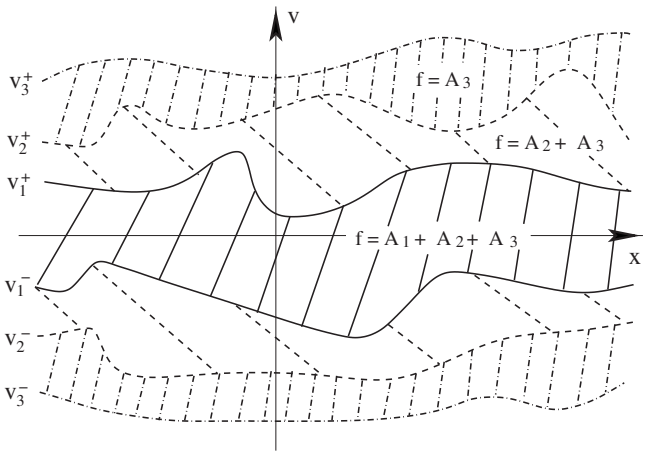

FIG. 1. Gyro-water-bag: Phase space plot for a three-bag model.

is an exact solution of the gyrokinetic Vlasov equation (4) in the sense of distribution theory, if and only if the set of the following equations are satisfied:

$$\partial_t v^\pm_{\mu j} + \mathcal{J}_\mu \mathbf{v}_E \cdot \nabla_\perp v^\pm_{\mu j} + v^\pm_{\mu j} \partial_z v^\pm_{\mu j} = \frac{q_i}{m_i} \mathcal{J}_\mu E_\parallel, \qquad (7)$$

for all $j \in [1, \mathcal{N}]$ and $\mu \in \Xi$. The quasineutrality coupling can be rewritten as

$$-\nabla_\perp \cdot \left(\frac{n_{i0}}{B\Omega_0} \nabla_\perp \phi \right) + \frac{e\tau n_{i0}}{T_{i0}} (\phi - \lambda \langle \phi \rangle_{\mathcal{M}}) = 2\pi \sum_{\mu \in \Xi} \sum_{j=1}^{\mathcal{N}} \mathcal{A}_{\mu j} \frac{\Omega_i}{q_i} \mathcal{J}_\mu (v^+_{\mu j} - v^-_{\mu j}) - n_{i0}. \qquad (8)$$

C. Using water-bag Liouville invariants to reduce phase space dimension

In Eq. (7), j is nothing but a label since no differential operation is carried out on the variable $v_\parallel$. What we actually do is to bunch together particles within the same bag j and let each bag evolve using the contour equation (7). Of course, the different bags are coupled through the quasineutrality equation.

This operation appears as an exact reduction of the phase space dimension (elimination of the velocity variable) in the

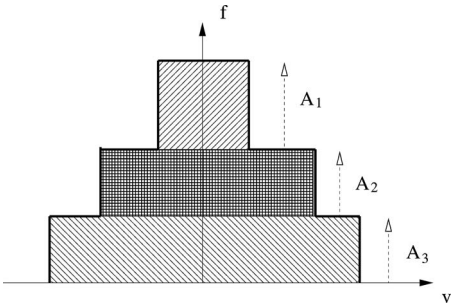

FIG. 2. Gyro-water-bag: Distribution function for a three-bag model.

sense that the water-bag concept makes full use of the Liouville invariance in phase space: The fact that $A_{\mu j}$ are constant in time is nothing but a straightforward consequence of the Vlasov conservation $Df/Dt=0$. Of course, the eliminated velocity reappears in the various bags j ($j=1,\ldots,\mathcal{N}$), and if we need a precise description of a continuous distribution a large $\mathcal{N}$ is needed. On the other hand, there is no mathematical lower bound on $\mathcal{N}$ and from a physical point of view many interesting results can even be obtained with $\mathcal{N}$ as small as 1 for electrostatic plasma. For magnetized plasma, $\mathcal{N}=2$ or 3 allow more analytical approaches [32].

On the contrary, in the Vlasov phase space $(\mathbf{r},v_\parallel)$, the exchange of velocity is described by a differential operator. From a numerical point of view, this operator must be approximated by some finite-difference scheme. Consequently, a minimum size for the mesh in the velocity space is required and we are faced with the usual sampling problem. If it can be claimed that the $v_\parallel$ gradients of the distribution function remain weak enough for some class of problems, then a rough sampling might be acceptable. However, it is well known in kinetic theory that wave-particle interaction is often not so obvious. For instance, steep gradients in the velocity space can be the signature of strong wave-particle interaction and there is the need for a higher numerical resolution of Vlasov code, while a water-bag description can still be used with a small bag number. As a matter of fact it is well known that this mesh problem is closely related to poor entropy conservation (see, for instance, [33]).

To conclude, the gyro-water-bag offers an exact description of the plasma dynamics even with a small bag number, allowing more analytical studies and bringing the link between the hydrodynamic description and full Vlasov one. Of course this needs a special initial preparation of the plasma (Lebesgue subdivision). Furthermore, there is no constraint on the shape of the distribution function which can be very far from a Maxwellian. Once initial data has been prepared using Lebesgue subdivision, the gyro-water-bag equations give the exact weak (in the sense of the theory of distribution) solution of the Vlasov equation corresponding to this initial data. Any initial condition (continuous or not) which is integrable with respect to the Lebesgue measure can be approximated accurately with larger $\mathcal{N}$. Therefore, if we need a precise description of a continuous distribution, it is clear that a larger $\mathcal{N}$ is needed; but even if the numerical effort is close to a standard discretization of the velocity space in a regular Vlasov code (using $2\mathcal{N}+1$ mesh points), we believe that the use of an exact water-bag sampling should give better results than approximating the corresponding differential operator.

D. Linking kinetic and fluid descriptions

Let us introduce for each bag j the density $n_{\mu j}=(v^+_{\mu j}-v^-_{\mu j})\mathcal{A}_{\mu j}$ and the average velocity $u_{\mu j}=(v^+_{\mu j}+v^-_{\mu j})/2$. After some algebra, Eq. (7) leads to continuity and Euler equations, namely

$$\partial_t n_{\mu j}+\nabla_\perp\cdot(n_{\mu j}\mathcal{J}_\mu\mathbf{v}_\mathbf{E})+\partial_z(n_{\mu j}u_{\mu j})=0,$$

$$\partial_t(n_{\mu j}u_{\mu j})+\nabla_\perp\cdot(n_{\mu j}u_{\mu j}\mathcal{J}_\mu\mathbf{v}_\mathbf{E})+\partial_z(n_{\mu j}u^2_{\mu j})+\frac{1}{m_i}\partial_z p_{\mu j}=\frac{q_i}{m_i}n_{\mu j}\mathcal{J}_\mu E_\parallel,$$

where the partial pressure takes the form $p_{\mu j}=m_i n^3_{\mu j}/(12\mathcal{A}^2_{\mu j})$. The connection between kinetic and fluid description clearly appears in the previous multifluid equations. The case of one bag recovers a fluid description (with an exact adiabatic closure with $\gamma=3$). Consequently, the gyro-water-bag provides a fully kinetic description which is shown to be equivalent to a multifluid one.

Actually each bag is a fluid described by Euler's equations with a specific adiabatic closure while the coupling between all the fluids is given by the quasineutrality equation (8). The sum over the bags in (8) allows us to recover the kinetic character from a set of fluid equations. For example, in the more simple electrostatic Vlasov-Poisson plasma [16,17,21–23,32], the well-known Landau damping is recovered by a phase-mixing process of $\mathcal{N}$ discrete undamped fluid eigenmodes which is reminiscent of the Van Kampen-Case treatment [34,35]. The linearized water-bag model is nothing but the "discrete" version of the continuous Van Kampen eigenmodes of the linearized Vlasov-Poisson system.

III. WEAK TURBULENCE THEORY OF THE GYRO-WATER-BAG MODEL

As shown above, the gyro-water-bag provides a simplification of the gyrokinetic description by simply solving a finite set of contour convective equations (7). These contour equations are intrinsically simpler than kinetic ones since they involve only the real space without having to cope with velocity resonance leading to complex analytical continuation. Actually the kinetic character is recovered by some phase-mixing process due to the coupling between all the bags provided by the quasineutrality equation (8).

As a first step, the linearized version of gyro-water-bag equations and the linear stability study of ITG modes have been extensively developed in a previous paper [32] which clearly demonstrates the "good properties" of the gyro-water-bag in the sense described above. It is the aim of this paper to go beyond the linear theory and use the analytical facilities of the gyro-water-bag to help at the understanding of the nature of the radial transport. To this purpose we suggest to derive radial transport equations through a quasilinear analysis, revealing the diffusive nature of the transport. It is important to point out that the water-bag concept (i.e., phase space conservation) is not affected by adding finite Larmor radius or curvature terms, except of course, for a more complicated algebra. As a result, to improve the comprehension and simplify the algebra we focus on what is physically important by assuming the asymptotic limit $k_\perp\rho_i\to 0$ (drift kinetic limit, $\mathcal{J}_\mu\to 1$) which does not remove generality of the method but suppresses $O(k^2_\perp\rho^2_i)$ order regularizing terms. In order to make the linear and quasilinear analysis [36–41] of Eqs. (7) and (8), each physical quantity $f\in\{v^\pm_j,\phi\}$ is expanded as a sum of the slowly time-evolving (θ,z)-uniform

state f_0 and a small first-order fluctuating perturbation δf such that $f(t,r,\theta,z)=f_0(t,r)+\delta f(t,r,\theta,z)$, where

$$\delta f(t,r,\theta,z)=\sum_{(m,n)\neq 0} f_{mn}(t,r)e^{i(k_\parallel z+m\theta)} \tag{9}$$

with $k_\parallel=2\pi n/L_z$, and $k_\theta=m/r$. Let us note that $\langle \delta f\rangle_{\theta,z}=0$, $\langle f_0\rangle_{\theta,z}=f_0$, where $\langle\cdot\rangle_{\theta,z}$ denotes (θ,z) averaging, and $f_{-m,-n}=\bar{f}_{mn}$.

A. First-order equations

Let us find the equations for the slowly evolving part $(\{v_{j0}^\pm\}_{j\in[1,\mathcal{N}]},\phi_0)$. If we perform the (θ,z) average of Eq. (7) we obtain

$$\partial_t v_{j0}^\pm-\frac{1}{rB}\langle \partial_\theta\delta\phi\partial_r\delta v_j^\pm-\partial_r\delta\phi\partial_\theta\delta v_j^\pm\rangle_{\theta,z}=0. \tag{10}$$

Using Fourier expansion (9), Eq. (10) becomes

$$\partial_t v_{j0}^\pm+\frac{i}{r}\partial_r\left(r\sum_{(m,n)\neq 0}\frac{k_\theta}{B}\bar{\phi}_{mn}v_{jmn}^\pm\right)=0. \tag{11}$$

Performing the (θ,z) average of Eq. (8) and setting $\chi_0=1/(rn_{i0})$, yields the equation for the zonal flow ϕ_0,

$$-\chi_0\partial_r\left(\frac{\partial_r\phi_0}{\chi_0}\right)+\frac{eB\Omega_0}{k_BT_{e0}}(1-\lambda)\phi_0=\frac{\Omega_0B}{n_{i0}}\left(\sum_{j\leq\mathcal{N}}\mathcal{A}_j(v_{j0}^+-v_{j0}^-)-n_{i0}\right). \tag{12}$$

If we subtract (11) from (7) and (12) from (8), by neglecting second-order terms in the perturbation we obtain the following equations for the first-order perturbation part:

$$\partial_t v_{jmn}^\pm+i\mathbf{k}\cdot\mathbf{V}_{j0}^\pm v_{jmn}^\pm+i\phi_{mn}\lambda_{j0}^\pm=0 \tag{13}$$

and

$$-\chi_0\partial_r\left(\frac{\partial_r\phi_{mn}}{\chi_0}\right)+\left(\frac{eB\Omega_0}{k_BT_{e0}}+\frac{m^2}{r^2}\right)\phi_{mn}=\frac{\Omega_0B}{n_{i0}}\sum_{j\leq\mathcal{N}}\mathcal{A}_j(v_{jmn}^+-v_{jmn}^-), \tag{14}$$

where $\mathbf{k}=(k_\parallel,k_\theta)^T$ and

$$\mathbf{V}_{j0}^\pm=\left(v_{j0}^\pm,\frac{\partial_r\phi_0}{B}\right)^T,\quad \lambda_{j0}^\pm=\frac{q_i}{m_i}k_\parallel-\frac{k_\theta}{B}\partial_r v_{j0}^\pm.$$

The integration of Eq. (13) gives

$$v_{jmn}^\pm(t)=v_{jmn}^\pm(0)\exp\left(-i\int_0^t\mathbf{k}\cdot\mathbf{V}_{j0}^\pm(s)ds\right)-i\int_0^t ds\,\phi_{mn}(t-s)\lambda_{j0}^\pm(t-s)\times\exp\left(-i\int_{t-s}^t\mathbf{k}\cdot\mathbf{V}_{j0}^\pm(\tau)d\tau\right). \tag{15}$$

We now look for solution of the form Wentzel-Kramers-Brillouin (WKB ansatz)

$$f_{mn}(t,r)=\tilde{f}_{mn}(t,r)e^{-i\omega_{mn}t}, \tag{16}$$

where the phase $\omega_{mn}=\omega_{\mathbf{k}}$ is a real number such that $\omega_{-m,-n}=\omega_{-\mathbf{k}}=-\omega_{\mathbf{k}}=-\omega_{mn}$, and where the envelope function $\tilde{f}_{mn}(t)$ is a time slowly varying real function on a time scale such as $\gamma_{\mathbf{k}}^{-1}$. Here $\gamma_{\mathbf{k}}$ is the growth rate of the ITG instability and τ_{dif} is the time scale of the variation of $v_{j0}^\pm$ (due to the diffusion). The time scale of the fluctuating envelope is greater than the time scale of the fluctuation oscillation $\tau_{fo}\sim\omega_{\mathbf{k}}^{-1}$, therefore, we have $|\gamma_{\mathbf{k}}/\omega_{\mathbf{k}}|\ll 1$. For the sake of clarity we drop the tilde notation in the sequel of the paper. The first term on the right-hand side of (15), the free-streaming part of the solution, rapidly damps because of the phase mixing (see [40] for more details) in the j summation or $v_\parallel$ integration on a time $\tau_d\sim(k_\parallel\bar{v})^{-1}$, where $\bar{v}$ is the characteristic spread in the parallel velocity, i.e., the parallel thermal velocity. Provided that $t\gg\tau_d$ we can drop the initial value term of (15). Thus, plugging (15) into (14) yields

$$-\chi_0\partial_r\left(\frac{\partial_r\phi_{mn}}{\chi_0}\right)+K\phi_{mn}=-iL\int_0^t C(t,s)\phi_{mn}(t-s)ds, \tag{17}$$

where $K=m^2/r^2+eB\Omega_0/(k_BT_{e0})$, $L=\Omega_0B/n_{i0}$, and

$$C(t,s)=\sum_{j\leq\mathcal{N}}\mathcal{A}_j\left[\lambda_{j0}^+(t-s)\exp\left(i\int_{t-s}^t\Omega_{j0}^+(\tau)d\tau\right)-\lambda_{j0}^-(t-s)\exp\left(i\int_{t-s}^t\Omega_{j0}^-(\tau)d\tau\right)\right]$$

with $\Omega_{j0}(\tau)^\pm=\omega-\mathbf{k}\cdot\mathbf{V}_{j0}^\pm(\tau)$ as the Doppler shifted pulsation. Once again by phase-mixing arguments, the sum over j leads to the decay of $C(t,s)$ with s on a time τ_d. If this time is short compared to τ_{dif}—the evolution time of $(\{v_{j0}^\pm\}_{j\in[1,\mathcal{N}]},\phi_0)$—(due to the diffusion) and to $\gamma_{\mathbf{k}}^{-1}$—the evolution time of ϕ_{mn}—we may Taylor expand $\lambda_{j0}^\pm$, $\mathbf{V}_{j0}^\pm$, and ϕ_{mn}

$$\lambda_{j0}^\pm(t-s)=\lambda_{j0}^\pm(t)-\dot{\lambda}_{j0}^\pm(t)s+O(s^2),$$

$$\int_{t-s}^t\mathbf{k}\cdot\mathbf{V}_{j0}^\pm(\tau)d\tau=\mathbf{k}\cdot\mathbf{V}_{j0}^\pm(t)s+O(s^2),$$

$$\phi_{mn}(t-s)=\phi_{mn}(t)-s\dot{\phi}_{mn}(t)+O(s^2). \tag{18}$$

From Eq. (17) and Taylor expansions (18), using

$$\int_0^\infty e^{i\omega s}ds=\pi\delta(\omega)+i\mathcal{P}(\omega)=\delta_+(\omega),$$

where $\mathcal{P}(\cdot)$ is the principal-value distribution $\mathrm{P}(1/\cdot)$, and neglecting all terms of second order in s we obtain

$$-\chi_0\partial_r\left(\frac{\partial_r\phi_{mn}}{\chi_0}\right)+K\phi_{mn}=-iL\sum_{j\leq\mathcal{N}}\mathcal{A}_j\{\phi_{mn}(t)[\lambda_{j0}^+\delta_+(\Omega_{j0}^+)-\lambda_{j0}^-\delta_+(\Omega_{j0}^-)]+i\dot{\phi}_{mn}\partial_\omega[\lambda_{j0}^+\delta_+(\Omega_{j0}^+)-\lambda_{j0}^-\delta_+(\Omega_{j0}^-)]$$

$$+ i\phi_{mn}\partial_\omega[\dot{\lambda}^+_{j0}\delta_+(\Omega^+_{j0}) - \dot{\lambda}^-_{j0}\delta_+(\Omega^-_{j0})]\}. \quad (19)$$

Supposing that $\tau_{\rm dif} \gg \gamma_{\mathbf{k}}^{-1}$ the third term on the right-hand side of (19) can be neglected and using the notation $\delta^\pm_{+j} = \delta_+(\Omega^\pm_{j0})$ we obtain

$$\dot{\phi}_{mn}\left(L\sum_{j\le\mathcal{N}}\mathcal{A}_j\partial_\omega(\lambda^+_{j0}\delta^+_{+j} - \lambda^-_{j0}\delta^-_{+j})\right) - \chi_0\partial_r\left(\frac{\partial_r\phi_{mn}}{\chi_0}\right)$$
$$-\left(K + iL\sum_{j\le\mathcal{N}}\mathcal{A}_j(\lambda^+_{j0}\delta^+_{+j} - \lambda^-_{j0}\delta^-_{+j})\right)\phi_{mn} = 0. \quad (20)$$

To lowest order in $\dot{\phi}_{mn}$, the real part of (20) gives the dispersion relation $\epsilon(\mathbf{k},\omega_{\mathbf{k}})=0$ with

$$\left(K - L\sum_{j\le\mathcal{N}}\mathcal{A}_j[\lambda^+_{j0}\mathcal{P}(\Omega^+_{j0}) - \lambda^-_{j0}\mathcal{P}(\Omega^-_{j0})]\right)\phi_{mn} - \chi_0\partial_r\left(\frac{\partial_r\phi_{mn}}{\chi_0}\right)$$
$$= \epsilon(\mathbf{k},\omega_{\mathbf{k}}). \quad (21)$$

The imaginary part of (20) gives the growth rate $\gamma_{\mathbf{k}} = \dot{\phi}_{mn}/\phi_{mn}$,

$$\gamma_{\mathbf{k}} = \frac{\pi\sum_{j\le\mathcal{N}}\mathcal{A}_j[\lambda^+_{j0}\delta(\Omega^+_{j0}) - \lambda^-_{j0}\delta(\Omega^-_{j0})]}{\partial_\omega\sum_{j\le\mathcal{N}}\mathcal{A}_j[\lambda^+_{j0}\mathcal{P}(\Omega^+_{j0}) - \lambda^-_{j0}\mathcal{P}(\Omega^-_{j0})]}. \quad (22)$$

B. Quasilinear analysis

We now follow the analysis by introducing $\delta^2 v_j^\pm$, the second-order perturbation in $v_j^\pm$, such that $\langle\delta^2 v_j^\pm\rangle_{\theta,z} \neq 0$. We then plug in the expansion $v_j^\pm = v_{j0}^\pm + \delta v_j^\pm + \delta^2 v_j^\pm$ and use the WKB ansatz (16) into Eqs. (11) and (15). The first term on the right-hand side of (15), the free-streaming part of the solution, will rapidly damp in (11) because of the phase mixing in the $\mathbf{k}$ integration on a time $\tau_{fs} \sim |\Delta(\omega_{\mathbf{k}} - \mathbf{k}\cdot\mathbf{V}^\pm_{j0})|^{-1} \sim |\Delta\mathbf{k}\cdot(\frac{\partial\omega_{\mathbf{k}}}{\partial\mathbf{k}} - \mathbf{V}^\pm_{j0})|^{-1}$ provided that

(i) the Fourier transform of the initial condition $\{v_j^\pm(0)\}_{j\in[1,\mathcal{N}]}$ and the electrical potential ϕ are smooth functions in $\mathbf{k}$.

(ii) We have $\frac{\partial\omega_{\mathbf{k}}}{\partial\mathbf{k}} \neq \mathbf{V}^\pm_{j0}$.

(iii) We have $|\Delta(\omega_{\mathbf{k}} - \mathbf{k}\cdot\mathbf{V}^\pm_{j0})|^{-1} \ll \gamma_{\mathbf{k}}^{-1}, \tau_{\rm dif}$.

In fact we have the following time ordering:

$$\tau_d, \tau_{fo} \sim \omega_{\mathbf{k}}^{-1}, \tau_{fs}, \tau_{ac} \ll \gamma_{\mathbf{k}}^{-1}, \tau_{\rm dif}, \tau_D \ll \tau_{tr} = \omega_b^{-1},$$

where τ_{ac}, is the wave autocorrelation time ($\tau_{ac} \sim \tau_{fs}$ for resonant particles), τ_D is the Dupree time [41], i.e., the particle decorrelation time, and $\tau_{tr} = \omega_b^{-1}$ is the trapping time or the inverse of the bounce frequency associated with this typical wave of the electric field disturbance. Actually this quasilinear analysis is justified for $\tau_{\rm dif} \lesssim \tau_D$ only. Dropping the free-streaming term because phase mixing leads to its decay on a time τ_{fs}, after (θ,z) averaging and neglecting third-order terms in the perturbation, we obtain

$$\partial_t v^\pm_{j0} + \partial_t\langle\delta^2 v_j^\pm\rangle_{\theta,z} + \frac{1}{r}\partial_r\left(r\int_0^t \lambda^\pm_{j0}(t-s)\mathcal{K}^\pm(t,s,\mathbf{V}^\pm_{j0})ds\right) = 0, \quad (23)$$

where

$$\mathcal{K}^\pm(t,s,\mathbf{V}^\pm_{j0}) = \sum_{(m,n)\neq 0}\frac{k_\theta}{B}\phi_{mn}(t-s) \times\bar{\phi}_{mn}(t)\exp\left(i\int_{t-s}^t \Omega^\pm_{j0}(\tau)d\tau\right).$$

Again by phase mixing the sum over the couple (m,n) or $\mathbf{k}$ integration in expression (23) leads to the decay of $\mathcal{K}^\pm$ in s on time τ_{fs}, and when this time is shorter than $\gamma_{\mathbf{k}}^{-1}$ we may use (18). Moreover, assuming the ordering $\tau_{\rm dif} \gg \gamma_{\mathbf{k}}^{-1}$, Eq. (23) becomes

$$\partial_t v^\pm_{j0} + \partial_t\langle\delta^2 v_j^\pm\rangle_{\theta,z} + \frac{1}{r}\partial_r(\mathcal{J}^\pm) = 0 \quad (24)$$

with

$$\mathcal{J}^\pm_j(t) = r\int_0^\infty \lambda^\pm_{j0}(t-s)\mathcal{K}^\pm(t,s,\mathbf{V}^\pm_{j0})ds$$
$$= \sum_{(m,n)\neq 0}\int_0^\infty \frac{rk_\theta}{B}\lambda^\pm_{j0}(t) \times\left(|\phi_{mn}(t)|^2 - \frac{s}{2}\frac{d}{dt}|\phi_{mn}(t)|^2\right)e^{is\Omega^\pm_{j0}}ds$$
$$= \sum_{(m,n)\neq 0}\frac{rk_\theta}{B}\lambda^\pm_{j0}(t) \times\left(|\phi_{mn}(t)|^2 + \frac{1}{2}\frac{d}{dt}|\phi_{mn}(t)|^2 i\partial_\omega\right)\delta_+(\Omega^\pm_{j0}), \quad (25)$$

where the extension of the s integration to infinity is justified by the decay of $\mathcal{K}^\pm$ in s. Let us now make the index decomposition $\mathbb{Z}^{2*} = \mathbb{D}\oplus\mathbb{D}^c$ where $\mathbb{D} = \{\nu = (m,n) | m > 0\}$ and $\mathbb{D}^c$ is the complementary of the set $\mathbb{D}$. Therefore (25) becomes

$$\mathcal{J}^\pm_j = \sum_{\nu\in\mathbb{D}}\frac{rk_\theta}{B}\lambda^\pm_{j0}\left(|\phi_\nu|^2 2\pi\delta(\Omega^\pm_{j0}) - \frac{d}{dt}|\phi_\nu|^2\partial_\omega\mathcal{P}(\Omega^\pm_{j0})\right). \quad (26)$$

C. Obtaining a reaction-diffusion model

Finally we substitute the expression (26) into (24) and associated, respectively, the first term of the right-hand side of (26) to $\partial_t v^\pm_{j0}$ and the second term on the right-hand side of (26) to $\partial_t\langle\delta^2 v_j^\pm\rangle_{\theta,z}$. Therefore, $\partial_t v^\pm_{j0}$ satisfies a Fokker-Planck equation with a nonlinear source term

$$\frac{\partial v^\pm_{j0}}{\partial t} = \frac{1}{r}\frac{\partial}{\partial r}\left(\mathcal{F}^\pm_j v^\pm_{j0} + \mathcal{D}^\pm_j\frac{\partial v^\pm_{j0}}{\partial r}\right) + \frac{1}{r}\frac{\partial}{\partial r}\left(Q^\pm_j\frac{\partial\phi_0}{\partial r}\right) \quad (27)$$

with resonant positive diffusion coefficients

$$\mathcal{D}_j^{\pm} = 2\pi r \sum_{\nu\in\mathbb{D}} \left(\frac{k_\theta}{B}\right)^2 |\phi_\nu|^2 \delta(\omega_{\mathbf{k}} - \mathbf{k}\cdot\mathbf{V}_{j0}^{\pm}),$$

friction coefficients

$$\mathcal{F}_j^{\pm} = \sum_{\nu\in\mathbb{D}} \mathcal{G}_{j\nu}^{\pm}(1+\mathcal{I}_{j\nu}^{\pm})|\phi_\nu|^2 \delta(\omega_{\mathbf{k}} - \mathbf{k}\cdot\mathbf{V}_{j0}^{\pm}),$$

and source coefficients

$$\mathcal{Q}_j^{\pm} = \sum_{\nu\in\mathbb{D}} \mathcal{G}_{j\nu}^{\pm}\mathcal{I}_{j\nu}^{\pm}\frac{k_\theta}{k_\parallel B}|\phi_\nu|^2 \delta(\omega_{\mathbf{k}} - \mathbf{k}\cdot\mathbf{V}_{j0}^{\pm}),$$

where $\mathcal{G}_{j\nu}^{\pm} = -(2\pi r q_i k_\theta k_\parallel^2)/(m_i B\mathbf{k}\cdot\mathbf{V}_{j0}^{\pm})$ and $\mathcal{I}_{j\nu}^{\pm} = (k_\theta \partial_r \phi_0)/(B\mathbf{k}\cdot\mathbf{V}_{j0}^{\pm})$.

Let us note that the bags are coupled by the equation of the zonal flow (12). Equation (27) for the radial transport reveals the diffusive nature of the transport in the radial direction which is, indeed, a well-known fact. Equation (27) with $\mathcal{Q}_j^{\pm}=0$ expresses the radial diffusion of each bag independently. Now, the existence of the source term due to $\mathcal{Q}_j^{\pm}$ in (27) couples the bags dynamics with the zonal flow ϕ_0 given self-consistently by Eq. (12). Consequently, the system (12) and (27) is a reaction-diffusion model describing the weak-turbulence diffusion (direct energy cascade) which enters in competition with the back reaction driven by the nonlinear diffusion term [last term in (27)] on the mean-zonal-flow (inverse energy cascade).

The present model, through the introduction of the water-bag within the multifluid "Lebesgue" decomposition, provides a kinetic generalization of the usual fluid prescription in a magnetized plasma. In such a plasma, if flow shear exists together with density-temperature (or pressure) gradient, a source of the turbulence, the flow shear may suppress the turbulence driven by pressure gradient relaxation. These shear flows can be self-generated, in which case the Reynolds stress tensor is their main driving term. There is an energy transfer from the turbulent low-frequency electromagnetic (drift waves) fluctuations to these periodic zonal flow fluctuations via either local (inverse energy cascade) or nonlocal interactions in Fourier space. The back reaction of self-generated shear flow, on pressure-gradient-driven turbulence, is a key mechanism that governs the turbulent state and the transport, especially it can lead to the formation of transport barriers. In fact many nonlinear simulations show a significant reduction of the transport when zonal flows are present [7,8,42]. In a review of zonal flow phenomena [43], it is shown that poloidal velocity shear plays an important role in regulating (suppressing) turbulent transport. In that case the back reaction of shear flows on turbulence can take the form of random shearing on turbulent eddies, leading to a diffusion of drift waves action in the wave-number space k_r. In other words, the drift wave spectrum in k_r spreads diffusively.

Furthermore, our model seems, indeed, to have some universal properties for the reaction-diffusion process. In the one-bag case, with $v^+=v^-$ (zero temperature limit), Eqs. (12) and (27) have the same mathematical structure as ones encountered in chemotaxis models—namely the Keller-Segel model [44]—to describe the collective transport (diffusion, concentration, and aggregation) of cells attracted by a self-emitted chemical substance in biological multicellular organisms. In this picture the bags play the role of the density of different cell groups and the zonal flow, through the mean electrical potential, plays the role of the chemoattractant.

Finally the superposition of several bags, as $\mathcal{N}$ undamped eigenmodes, allows us to recover kinetic features (nonlinear resonant wave-particle interaction) of the phase-space flow by the phase-mixing process of real frequencies leading to gyrokinetic turbulence.

D. Conservation laws

If we now integrate the equation on $\langle \delta^2 v_j^{\pm}\rangle_{\theta,z}$ we obtain

$$\langle \delta^2 v_j^{\pm}\rangle_{\theta,z} = \frac{1}{r}\partial_r \sum_{\nu\in\mathbb{D}} \frac{r k_\theta}{B}\lambda_{j0}^{\pm}|\phi_\nu|^2 \partial_{\omega_{\mathbf{k}}}\mathcal{P}(\Omega_{j0}^{\pm}). \tag{28}$$

As we will see below the term $\langle \delta^2 v_j^{\pm}\rangle_{\theta,z}$ yields the wave momentum and the particle contribution to energy density. We now show that the density, momentum, and energy are conserved at second order in the perturbation. Using Eq. (27), after integrating over the cylinder we obtain easily the conservation of the total density,

$$\frac{dn_0}{dt} = \frac{d}{dt}\sum_{j\le\mathcal{N}} \mathcal{A}_j \int r dr (v_{j0}^+ - v_{j0}^-) = 0.$$

Let us now compute

$$\frac{d}{dt}(I_0+I_2) = \frac{d}{dt}\left(\frac{1}{2}\sum_{j\le\mathcal{N}}\mathcal{A}_j\int r dr (v_{j0}^{+2} - v_{j0}^{-2}) + \sum_{j\le\mathcal{N}}\mathcal{A}_j\int r dr (v_{j0}^+\langle\delta^2 v_j^+\rangle_{\theta,z} - v_{j0}^-\langle\delta^2 v_j^-\rangle_{\theta,z})\right).$$

Using Eqs. (27) and (28), after some algebra we obtain

$$\frac{d}{dt}(I_0+I_2) = \int dr \sum_{\nu\in\mathbb{D}} 2\pi \frac{r k_\theta}{B}|\phi_\nu|^2 \partial_r \Theta \Xi(\delta) - \int dr \sum_{\nu\in\mathbb{D}} \frac{r k_\theta}{B}\frac{d|\phi_\nu|^2}{dt}\partial_\omega[\partial_r\Theta\Xi(\mathcal{P})]$$

with $\Theta = \frac{\omega}{k_\parallel} - \frac{\partial_r\phi_0 k_\theta}{B k_\parallel}$ and

$$\Xi(f) = \sum_{j\le\mathcal{N}} \mathcal{A}_j[\lambda_{j0}^+ f(\Omega_{j0}^+) - \lambda_{j0}^- f(\Omega_{j0}^-)],$$

where f denotes a generic one-dimensional distribution. Finally using (22) we obtain

$$\frac{d}{dt}(I_0+I_2) = 0,$$

which means that the momentum is conserved at second order in the perturbation $\delta v_j^{\pm}$. Let us now compute

$$\frac{d}{dt}(K_0+K_2)=\frac{d}{dt}\left(\frac{1}{3}\sum_{j\leq\mathcal{N}}\mathcal{A}_j\int rdr(v_{j0}^{+3}-v_{j0}^{-3})\right.$$
$$\left.+\sum_{j\leq\mathcal{N}}\mathcal{A}_j\int rdr(v_{j0}^{+2}\langle\delta^2 v_j^+\rangle_{\theta,z}-v_{j0}^{-2}\langle\delta^2 v_j^-\rangle_{\theta,z})\right).$$

Using Eqs. (27) and (28), after some algebra, we obtain

$$\frac{d}{dt}(K_0+K_2)=\int dr\sum_{\nu\in\mathbb{D}}2\pi\frac{rk_\theta}{B}|\phi_\nu|^2\partial_r\Theta^2\Xi(\delta)$$
$$-\frac{d}{dt}\int dr\sum_{\nu\in\mathbb{D}}\frac{rk_\theta}{B}|\phi_\nu|^2\partial_\omega[\partial_r\Theta^2\Xi(\mathcal{P})]. \tag{29}$$

Using the dispersion relation (21) the last term on the right-hand side of (29) becomes

$$-\frac{d\mathcal{E}_\phi}{dt}-\int dr\sum_{\nu\in\mathbb{D}}\frac{rk_\theta}{B}\frac{d|\phi_\nu|^2}{dt}\partial_r\Theta^2\partial_\omega\Xi(\mathcal{P}),$$

where $\mathcal{E}_\phi$ denotes the electrical potential energy. Finally using (22) and (29) we obtain

$$\frac{d}{dt}(K_0+K_2+\mathcal{E}_\phi)=\frac{d}{dt}(K_0+\mathcal{E})=0$$

which yields the conservation of the energy at second order in the perturbation $\delta v_j^\pm$. The term $\mathcal{E}$ stands for the total wave energy

$$\mathcal{E}=\int rdr\sum_{\nu\in\mathbb{D}}2\left(\frac{k_\theta}{Bk_\parallel}\right)^2\frac{\partial_r^2\phi_0}{L}\phi_\nu\omega\partial_\omega\epsilon.$$

IV. SELF-CONSISTENT QUASILINEAR GYRO-WATER-BAG CODE

In the preceding section we have derived a nonlinear reaction-diffusion model, using standard quasilinear time ordering assumption. The model is written in a formal way in order to allow further analytical studies: Whether this model is able to describe transport barrier, intermittency, the magnitude of zonal flow, anomalous heat transport, etc., are questions which will be addressed in a forthcoming paper. The most important question now is to check the quasilinear hypothesis through a full numerical solution of the gyro-water-bag equations (7) and (8).

A. Rewriting the gyro-water-bag equations

Since Eqs. (12) and (27) are formally written, they are not suited for direct numerical comparison with Eqs. (7) and (8). In this section we shall rewrite a quasilinear system suitable for numerical purpose. Every unknown is expanded as

$$f(t,r,\theta,z)=\frac{1}{2}f_0(t,r,z)+\frac{1}{2}\sum_{m>0}f_m(t,r,z)e^{i\theta m}+\text{c . c . ,} \tag{30}$$

where f_0 is a real number and f_m is a complex number. Introducing the expansion (30) into Eq. (7), where we assume the asymptotic limit $k_\perp\rho_i\to 0$ (drift kinetic limit, $\mathcal{J}_\mu\to 1$), after some algebra we obtain

$$\partial_t v_{j0}^\pm+\partial_z\left(\frac{v_{j0}^{\pm 2}}{2}+\phi_0\right)+\frac{1}{2rB}\sum_m m\partial_r(V_{jm}^\pm\times\Phi_m)$$
$$+\frac{1}{4}\sum_m\partial_z(|V_{jm}^\pm|^2)=0, \tag{31}$$

$$\partial_t V_{jm}^\pm+\frac{1}{r}\partial_r(r\mathcal{H}_m)V_{jm}^\pm-\frac{1}{r}\partial_r(r\mathcal{K}_{jm}^\pm)\Phi_m+\partial_z(v_{j0}^\pm V_{jm}^\pm+\Phi_m)+\mathcal{F}$$
$$=0, \tag{32}$$

where

$$\mathcal{H}_m=\frac{m}{Br}\phi_0\mathcal{I},\quad \mathcal{K}_{jm}^\pm=\frac{m}{Br}v_{j0}^\pm\mathcal{I},\quad \mathcal{I}=\begin{pmatrix}0&-1\\1&0\end{pmatrix},$$

$$V_{jm}^\pm=\begin{pmatrix}\text{Re } v_{jm}^\pm\\ \text{Im } v_{jm}^\pm\end{pmatrix},\quad \Phi_m=\begin{pmatrix}\text{Re } \phi_m\\ \text{Im } \phi_m\end{pmatrix},\quad \mathcal{F}=\begin{pmatrix}\mathcal{F}_1\\ \mathcal{F}_2\end{pmatrix}$$

with

$$\mathcal{F}_1=\frac{1}{2Br}\sum_\ell m(\partial_r\Phi_\ell\hat{\times}V_{jm-\ell}^\pm)+m(\partial_r\Phi_{m+\ell}\times V_{j\ell}^\pm)$$
$$+m(V_{jm+\ell}^\pm\times\partial_r\Phi_\ell)+\ell\partial_r(V_{jm+\ell}^\pm\times\Phi_\ell)$$
$$-(\ell+m)\partial_r(\Phi_{m+\ell}\times V_{j\ell}^\pm)-\ell\partial_r(\Phi_\ell\hat{\times}V_{jm-\ell}^\pm)$$
$$+\sum_\ell\frac{1}{4}\partial_z(V_{j\ell}^\pm\hat{\cdot}V_{jm-\ell}^\pm)+\frac{1}{2}\partial_z(V_{j\ell}^\pm\cdot V_{jm+\ell}^\pm) \tag{33}$$

and

$$\mathcal{F}_2=\frac{1}{2Br}\sum_\ell m(\partial_r\Phi_\ell\hat{\cdot}V_{jm-\ell}^\pm)+m(\partial_r\Phi_{m+\ell}\cdot V_{j\ell}^\pm)$$
$$+m(V_{jm+\ell}^\pm\cdot\partial_r\Phi_\ell)+\ell\partial_r(V_{jm+\ell}^\pm\cdot\Phi_\ell)$$
$$-(\ell+m)\partial_r(\Phi_{m+\ell}\cdot V_{j\ell}^\pm)-\ell\partial_r(\Phi_\ell\hat{\cdot}V_{jm-\ell}^\pm)$$
$$+\sum_\ell\frac{1}{4}\partial_z(V_{j\ell}^\pm\hat{\times}V_{jm-\ell}^\pm)+\frac{1}{2}\partial_z(V_{j\ell}^\pm\times V_{jm+\ell}^\pm). \tag{34}$$

In (33) and (34) we have used the notations $U\hat{\cdot}V=U_1V_1-U_2V_2$, $U\hat{\times}V=U_1V_2+U_2V_1$, where U and V are two-dimensional vectors. The quadratic nonlinear terms in $V_{jm}^\pm$, which lead to the coupling of modes and to the existence of a saturation regime will be neglected in (32) and kept in Eq. (31). In other words, the term $\mathcal{F}$ is dropped in (32). Using the dimensionless ordering parameters

$$\varepsilon_\delta=\frac{e\bar{\phi}}{k_B\bar{T}_0},\quad \varepsilon_k=\frac{k_\parallel}{k_\perp},\quad \varepsilon_\omega=\frac{\omega}{\Omega_0}=\frac{k_\parallel v_{thi}}{\Omega_0}, \tag{35}$$

Eqs. (31) and (32), in dimensionless form become

$$\partial_t v_{j0}^{\pm} + \partial_z\left(\frac{v_{j0}^{\pm 2}}{2} + Z_i \varepsilon_\delta \phi_0\right) + \sum_{m>0} \partial_z\left(\frac{|V_{jm}^{\pm}|^2}{4}\right) + \sum_{m>0} \eta_1 \frac{m}{2r} \partial_r (V_{jm}^{\pm} \times \Phi_m) = 0, \tag{36}$$

$$\partial_t V_{jm}^{\pm} + \eta_1 \frac{1}{r}[\partial_r (r\mathcal{H}_m) V_{jm}^{\pm} - \partial_r (r\mathcal{K}_{jm}^{\pm}) \Phi_m] + \partial_z (v_{j0}^{\pm} V_{jm}^{\pm} + Z_i \varepsilon_\delta \Phi_m) = 0, \tag{37}$$

where $\eta_1 = \varepsilon_\delta \varepsilon_\omega \varepsilon_k^{-2} Z_i$ and $B=1$ in the definition of $\mathcal{H}_m$ and $\mathcal{K}_{jm}^{\pm}$. Substituting the expansion (30) into Eq. (8) with the asymptotic limit $k_\perp \rho_i \to 0$ (drift kinetic limit, $\mathcal{J}_\mu \to 1$) and using the ordering dimensionless parameters (35) we obtain the dimensionless equations

$$-\eta_2 \frac{1}{r} \partial_r (r n_{i0} \partial_r \phi_0) + \frac{\varepsilon_\delta \tau n_{i0}}{T_{i0}} (\phi_0 - \lambda \langle \phi_0 \rangle_{\mathcal{M}}) = \sum_{j=1}^{\mathcal{N}} \mathcal{A}_j (v_{j0}^{+} - v_{j0}^{-}) - n_{i0} \tag{38}$$

and

$$-\eta_2 \frac{1}{r} \partial_r (r n_{i0} \partial_r \Phi_m) + \left(\eta_2 \frac{m^2}{r^2} + \frac{\varepsilon_\delta \tau n_{i0}}{T_{i0}}\right) \Phi_m = \sum_{j=1}^{\mathcal{N}} \mathcal{A}_j (V_{jm}^{+} - V_{jm}^{-}), \tag{39}$$

where $\eta_2 = \varepsilon_\delta \varepsilon_\omega^2 \varepsilon_k^{-2} Z_i$. Finally we are interested in solving the system formed by Eqs. (36)–(39).

B. Numerical method

This section is devoted to the numerical approximation of the system (36)–(39). To this aim we use the Runge-Kutta discontinuous Galerkin method [45]. We first depict the method for the transport equations (36) and (37). Let Ω be the domain of computation and $\mathcal{M}_h$ a partition of Ω of element K such that $\cup_{K \in \mathcal{M}_h} \bar{K} = \bar{\Omega}$, $K \cap Q = \varnothing$, $K, Q \in \mathcal{M}_h$, $K \neq Q$. We set $h = \max_{K \in \mathcal{M}_h} h_K$, where h_K is the exterior diameter of a finite element K. The first step of the method is to write Eqs. (36)–(39) in a variational form on any element K of the partition $\mathcal{M}_h$. Using a Green formula, for any enough regular test function φ, for all $j=1,\ldots,\mathcal{N}$, we consider the variational form of (36),

$$\partial_t \int_K dK v_{j0}^{\pm} \varphi - \frac{1}{2} \int_K dK v_{j0}^{\pm 2} \partial_z \varphi + \int_{\partial K} d\Gamma f(v_{j0}^{\pm}) n_{K,z} \varphi + Z_i \varepsilon_\delta \int_K dK \varphi E_{0z} - \eta_1 \sum_{m>0} m \left[\int_K dK V_{jm}^{\pm} \times \Phi_m \partial_r \left(\frac{\varphi}{2r}\right) - \int_{\partial K} d\Gamma V_{jm}^{\pm} \times \Phi_m n_{K,r} \frac{\varphi}{2r}\right] - \sum_{m>0} \left(\frac{1}{4} \int_K dK |V_{jm}^{\pm}|^2 \partial_z \varphi - \frac{1}{2} \int_{\partial K} d\Gamma [f(\mathrm{Re}\, V_{jm}^{\pm}) + f(\mathrm{Im}\, V_{jm}^{\pm})] n_{K,z} \varphi\right) = 0 \tag{40}$$

with

$$\int_K dK \varphi E_{0z} = -\int_K dK \phi_0 \partial_z \varphi + \int_{\partial K} d\Gamma \phi_0 n_{K,z} \varphi, \tag{41}$$

where ∂K denotes the boundary of K, n_K denotes the outward unit normal to ∂K, and $f(\cdot) = (\cdot)^2/2$. Let us introduce the notations $V_{jm}^{\pm} = (\mathrm{Re}\, V_{jm}^{\pm}, \mathrm{Im}\, V_{jm}^{\pm})^T = (V_{jm}^{\pm 1}, V_{jm}^{\pm 2})^T$, $\gamma_\alpha = (-1)^\alpha$, and $\beta = \mathrm{mod}(\alpha, 2) + 1$. Therefore, for $\alpha \in \{1,2\}$ and $j=1,\ldots,\mathcal{N}$, we consider the following variational form of Eqs. (37):

$$\partial_t \int_K dK V_{jm}^{\pm \alpha} \varphi - \int_K dK v_{j0}^{\pm} V_{jm}^{\pm \alpha} \partial_z \varphi + \eta_1 \int_K dK \frac{\gamma_\alpha m}{r} (E_{0r} V_{jm}^{\pm \beta} - \partial_r v_{j0}^{\pm} \Phi_m^\beta) \varphi + \int_{\partial K} d\Gamma v_{j0}^{\pm} V_{jm}^{\pm \alpha} n_{K,z} \varphi + Z_i \varepsilon_\delta \int_K dK E_{mz}^\alpha \varphi = 0, \tag{42}$$

where

$$\int_K dK \varphi E_{0r} = -\int_K dK \phi_0 \partial_r \varphi + \int_{\partial K} d\Gamma \phi_0 n_{K,r} \varphi, \tag{43}$$

$$\int_K dK \partial_r v_{j0}^{\pm} \varphi = -\int_K dK v_{j0}^{\pm} \partial_r \varphi + \int_{\partial K} d\Gamma v_{j0}^{\pm} n_{K,r} \varphi, \tag{44}$$

$$\int_K dK \varphi E_{mz}^\alpha = -\int_K dK \Phi_m^\alpha \partial_z \varphi + \int_{\partial K} d\Gamma \Phi_m^\alpha n_{K,z} \varphi. \tag{45}$$

We now seek an approximate solution ($v_{h,j0}^{\pm}$, Re $V_{h,jm}^{\pm}$, Im $V_{h,jm}^{\pm}$, $\phi_{h,0}$, Re $\Phi_{h,m}$, Im $\Phi_{h,m}$) whose restriction to the element K of the partition $\mathcal{M}_h$ of Ω belongs, for each value of the time variable, to the finite-dimensional local space $\mathcal{P}(K)$, typically a space of polynomials. Using the variational weak form (40)–(45) of the gyro-water-bag model (36) and (37) and the discontinuous Galerkin projection procedure (see Appendix A for more details), for all $K \in \mathcal{M}_h$, we obtain the ordinary differential equation (ODE),

$$\mathfrak{M} \frac{d}{dt} X_{h_{|K}} = \mathcal{L}_{K,X_h}(\{v_{h,j0_{|K'}}^{\pm}, V_{h,jm_{|K'}}^{\pm}, \phi_{h,0_{|K'}}, \Phi_{h,m_{|K'}} | \bar{K}' \cap \bar{K} \in \partial K\}),$$

where X_h denotes a generic unknown such that

$$X_h \in \Lambda = \{\{v_{h,j0}^{\pm}\}_{j \in [1,\mathcal{N}]}, \{V_{h,jm}^{\pm}\}_{j \in [1,\mathcal{N}], m>0}\}.$$

In the general case, the local mass matrix $\mathfrak{M}$ of low order [equal to the dimension of the local space $\mathcal{P}(K)$] is easily invertible. If we choose orthogonal polynomials the matrix $\mathfrak{M}$ is diagonal. Here we take Legendre polynomials as L^2-orthogonal basis function. Our code can run with Legendre polynomials of any degree, but for the numerical results exposed in the next section we choose polynoms of

degree 2. Moreover, we take a rectangular element $K=K_{pq}=\{(r,z)||r_p-r|\leq\Delta r/2,|z_q-z|\leq\Delta z/2\}$, where Δr and Δz are the space discretization parameters. Therefore, we must solve the ODE,

$$\frac{d}{dt}X_h = L_{h,X_h}(v^{\pm}_{h,j0}, V^{\pm}_{h,jm}, \phi_{h,0}, \Phi_{h,m}), \tag{46}$$

for all $X_h\in\Lambda$. In order to solve (46) we can use strong stability-preserving Runge-Kutta methods [46] (see Appendix B for more details). It now remains to solve the Helmholtz equations (38) and (39). If we set $\lambda=0$, Eqs. (38) and (39) take the general form

$$\partial_r\sigma+\chi\phi=\rho \quad \text{on } \Omega, \tag{47}$$

$$\varrho^{-1}\sigma=-\partial_r\phi \quad \text{on } \Omega, \tag{48}$$

$$\phi_{|r=r_{\min}}=0 \quad \text{or} \quad \partial_r\phi_{|r=r_{\min}}=0 \quad \forall \quad z\in\Omega_z, \tag{49}$$

$$\phi_{|r=r_{\max}}=0 \quad \forall \quad z\in\Omega_z, \tag{50}$$

$$\phi(r,z)=\phi(r,z+L_z) \quad \forall \quad r\in\Omega_r \tag{51}$$

with $\Omega=\Omega_r\times\Omega_z=[r_{\min},r_{\max}]\times[0,L_z]$. The term ρ/r stands for the right-hand side of (38) or (39), $\varrho(r)=\varepsilon_\delta\varepsilon_k^{-2}\varepsilon_\omega^2 Z_i r n_{i0}(r)$, and we define $\chi(r)=\varepsilon_\delta\tau r n_{i0}(r)/T_{i0}(r)$ for Eq. (38) or $\chi(r)=r\varepsilon_\delta\varepsilon_\omega^2\varepsilon_k^{-2}Z_i m^2/r^2+\varepsilon_\delta\tau r n_{i0}(r)/T_{i0}(r)$ for Eq. (39). In order to be consistent with the space discretization of the gyro-water-bag equations (36) and (37) we also solve the problem (47)–(51) within the framework of discontinuous Galerkin methods which leads to the inverse of a sparse linear system. For more details we refer the reader to Appendix C.

V. NUMERICAL RESULTS

A. Construction of a gyro-water-bag equilibrium

The first problem is to determine the physically relevant gyro-water-bag equilibrium which will be used to initialize the numerical scheme depicted previously. In order to describe ITG modes, we choose to construct radial profiles in terms of temperature and density profiles only. The continuous equilibrium distribution function is assumed as

$$f_{\rm eq}(r,v_\parallel)=\frac{n_{i0}(r)}{\sqrt{T_{i0}(r)}}\mathcal{F}\left(\frac{v_\parallel}{\sqrt{T_{i0}(r)}}\right), \tag{52}$$

where $n_{i0}(r)$ and $T_{i0}(r)$ are the normalized radial profiles of ion density and temperature. The function $\mathcal{F}$ is a normalized even function, thus for a local Maxwellian distribution, we obtain $\mathcal{F}(x)=\exp(-x^2/2)/\sqrt{2\pi}$. The first stage, will consist in constructing the gyro-water-bag model at $r=r_0$ and then extends it for all $r\in[r_{\min},r_{\max}]$. To this aim, as in [32], we use the method of equivalence between the radial derivatives of the moments of the stepwise gyro-water-bag and the radial derivatives of the corresponding continuous function. If we define, for $\ell=0,2,\ldots,2(\mathcal{N}-1)$, the r derivative of the ℓ momentum of $f_{\rm eq}$ as

$$\mathcal{M}_r^\ell(f_{\rm eq})=\int_{\mathbb{R}} dv_\parallel \partial_r f_{\rm eq}$$

and the r derivative of the ℓ momentum of the gyro-water-bag as

$$\mathcal{M}_r^\ell(\mathrm{GWB})=\sum_j^{\mathcal{N}} 2\mathcal{A}_j v_{j0}^\ell \partial_r v_{j0}$$

then, using integration by parts, the equality $\mathcal{M}_r^\ell(f_{\rm eq})=\mathcal{M}_r^\ell(\mathrm{GWB})$ at the point $r=r_0$ implies

$$\sum_j^{\mathcal{N}} \alpha_j(r_0)\Omega^\star_{v_{j0}}(r_0)[v_{j0}(r_0)]^\ell = \left(\Omega^\star_{n_{i0}}(r_0)+\frac{\ell}{2}\Omega^\star_{T_{i0}}(r_0)\right)[\sqrt{T_{i0}(r_0)}]^\ell\mathcal{M}^\ell(\mathcal{F}), \tag{53}$$

where $\mathcal{M}^\ell(\mathcal{F})$ is the ℓth-order moment of the function $\mathcal{F}$, $\alpha_j=2v_{j0}\mathcal{A}_j/n_{i0}$, $\Omega^\star_{v_{j0}}$ measure the local radial gradient of the bag v_{j0}, $\Omega^\star_{n_{i0}}$, and $\Omega^\star_{T_{i0}}$ are the diamagnetic frequencies defined by

$$\Omega^\star_{v_{j0}}=\frac{k_\theta T_{i0}}{q_i B}\frac{d\ln v_{j0}}{dr}=\frac{k_\theta T_{i0}}{q_i B}\kappa_{v_{j0}},$$

$$\Omega^\star_{n_{i0}}=\frac{k_\theta T_{i0}}{q_i B}\frac{d\ln n_{i0}}{dr}=\frac{k_\theta T_{i0}}{q_i B}\kappa_{n_{i0}},$$

$$\Omega^\star_{T_{i0}}=\frac{k_\theta T_{i0}}{q_i B}\frac{d\ln T_{i0}}{dr}=\frac{k_\theta T_{i0}}{q_i B}\kappa_{T_{i0}}.$$

We now introduce the unknown coefficients β_j and γ_j, for $j=1,\ldots,\mathcal{N}$, such that the constraint

$$\alpha_j\Omega_{v_{j0}}=\gamma_j\Omega^\star_{n_{i0}}+\tfrac{1}{2}\beta_j\Omega^\star_{T_{i0}} \tag{54}$$

is satisfied at the point $r=r_0$. If we substitute (54) into (53) then, the unknown gyro-water-bag parameters $(\alpha_j,\beta_j,\gamma_j)$ must satisfy the following linear system at the point $r=r_0$:

$$\sum_{1\leq j\leq\mathcal{N}}\alpha_j(r_0)[v_{j0}(r_0)]^\ell=(\ell+1)[\sqrt{T_{i0}(r_0)}]^\ell\mathcal{M}^\ell(\mathcal{F}), \tag{55}$$

$$\sum_{1\leq j\leq\mathcal{N}}\beta_j(r_0)[v_{j0}(r_0)]^\ell=\ell[\sqrt{T_{i0}(r_0)}]^\ell\mathcal{M}^\ell(\mathcal{F}), \tag{56}$$

$$\sum_{1\leq j\leq\mathcal{N}}\gamma_j(r_0)[v_{j0}(r_0)]^\ell=[\sqrt{T_{i0}(r_0)}]^\ell\mathcal{M}^\ell(\mathcal{F}). \tag{57}$$

Nevertheless in Eqs. (55)–(57) the matrix has the form of a Vandermonde system which becomes ill-conditioned for a great number of bags $\mathcal{N}$. A more convenient solution can be found for a large number of bags. Let us consider a regular sampling of the $v_\parallel$ axis, i.e., $v_{j0}(r_0)=(j-\frac{1}{2})\Delta v$, with $\Delta v=2v_{\max}/(2\mathcal{N}-1)$ and set $F_j=f_{\rm eq}[r_0,v_{j0}(r_0)-\frac{\Delta v}{2}]$. If we required that Eqs. (55)–(57) are satisfied at second order in Δv, then, using a trapeze quadrature rule to compute $\mathcal{M}^\ell(\mathcal{F})$, we obtain the solutions

$$\alpha_j(r_0) = 2\mathcal{A}_j \frac{v_{j0}(r_0)}{n_{i0}(r_0)} = 2(F_j - F_{j+1}) \frac{v_{j0}(r_0)}{n_{i0}(r_0)},$$

$$\gamma_j(r_0) = \Delta v \frac{F_j + F_{j+1}}{n_{i0}(r_0)}, \quad \beta_j(r_0) = \alpha_j(r_0) - \gamma_j(r_0).$$

Therefore gyro-water-bag parameters $\{\mathcal{A}_j\}_{j\in[1,\mathcal{N}]}$, and the initial condition for slowly time-evolving part $v_{j0}^{\pm}(t,r,z)$, for $j=1,\ldots,\mathcal{N}$, are given by

$$\mathcal{A}_j = F_j - F_{j+1}, \tag{58}$$

$$v_{j0}(r) = \sqrt{T_{i0}(r)}\mathcal{F}^{-1}\left(f_j \frac{\sqrt{T_{i0}(r)}}{n_{i0}(r)}\right), \tag{59}$$

$$v_{j0}^{\pm}(0,r,z) = \pm v_{j0}(r) \tag{60}$$

with $f_j = f_{\mathrm{eq}}[r_0, v_{j0}(r_0)]$. If we now differentiate (59) with respect to r, with $\mathcal{F}$ a normalized Maxwellian, we obtain

$$\kappa_{v_{j0}}(r) = \frac{1}{2}\kappa_{T_{i0}}(r)\left(1 - \frac{T_{i0}(r)}{v_{j0}^2(r)}\right) + \frac{T_{i0}(r)}{v_{j0}^2(r)}\kappa_{n_{i0}}(r) \tag{61}$$

which denotes that

$$\kappa_{v_{j0}} \sim O\left(\kappa_T, \kappa_n, \frac{1}{v_{j0}^2}\right),$$

and thus numerical problems could appear. If we keep a uniform $v_\parallel$ discretization to determine the gyro-water-bag equilibrium and if we want to use a large number of bags we see that $\kappa_{v_{10}}$ can explode as the first bag tends to zero. The radial profiles of the ion density and temperature are fixed in time and are deduced by integration of their gradient profiles

$$\kappa_{n_{i0}}(r) = \frac{1}{n_{i0}(r)}\frac{dn_{i0}(r)}{dr} = -\kappa_{n_{i0}}^0 \cosh^{-2}\left(\frac{r - r_0}{\Delta r_{n_{i0}}}\right),$$

$$\kappa_{T_{i0}}(r) = \frac{1}{T_{i0}(r)}\frac{dT_{i0}(r)}{dr} = -\kappa_{T_{i0}}^0 \cosh^{-2}\left(\frac{r - r_0}{\Delta r_{T_{i0}}}\right),$$

where r_0, $\kappa_{n_{i0}}^0$, $\kappa_{T_{i0}}^0$, $\Delta r_{n_{i0}}$, and $\Delta r_{T_{i0}}$ are free parameters. We next define the parameter $\eta(r) = d(\ln T_{i0})/d(\ln n_{i0})$ which determines locally if an ITG instability can develop ($\eta \geq 2$) or not ($\eta < 2$). The initial perturbation bag $V_{jm}^{\pm}(0)$ is chosen as

$$V_{jm}^{\pm}(0,r,z) = v_{j0}^{\pm}(0,r,z)p(r)\delta p(z),$$

where $p(r)$ is an even exponential function centered in r_0 such that $\lim_{r\to r_{\min}} p(r) = 0$ and $\lim_{r\to r_{\max}} p(r) = 0$. The perturbation δp is initialized with a cosine function with a single toroidal mode n or with a bath of modes

$$\delta p(z) = \sum_n \epsilon_n \cos\left(\frac{2\pi n}{L_z}z + \varphi_n\right),$$

where ϵ_n and φ_n represent, respectively, a random amplitude and a random phase for the mode n.

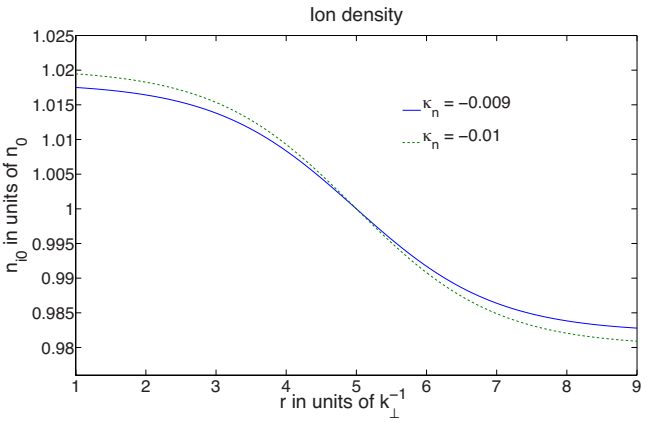

FIG. 3. (Color online) Initial ion density profile.

B. Normalization

The numerical scheme developed in Sec. IV B, is done using the normalized equations (36)–(39). In our case, the temperature T_{i0} and T_{e0} are normalized to $\bar{T}_0$, which is defined such that $T_{i0}(r_0)/T_0 = 1$. The longitudinal direction is normalized to $k_\parallel$, the characteristic fluctuation parallel wave number and the transversal direction to $k_\perp$, the characteristic fluctuation perpendicular wave number. The velocity is normalized to the ion thermal velocity $v_{thi} = \sqrt{T_{i0}/m_i}$ and the time to characteristic fluctuation frequency $\omega^{-1} = (k_\parallel v_{thi})^{-1}$. Finally the particle density n is normalized to $n_0 = \mathcal{A}v_{thi}$ and the electrical potential ϕ is normalized to the characteristic fluctuation potential $\bar{\phi}$. Moreover we define the dimensionless ordering parameters $\varepsilon_k = k_\parallel/k_\perp$, $\varepsilon_\omega = \omega/\Omega_0$, $\varepsilon_\delta = e\bar{\phi}/(k_B\bar{T}_0)$, $\varepsilon_{\nabla_{\mathrm{eq}}} = \rho_i/L_{\nabla_{\mathrm{eq}}}$, and $\varepsilon_\perp = \rho_i k_\perp$, where ρ_i is ion Larmor radius and $L_{\nabla_{\mathrm{eq}}}$ is the characteristic background plasma density and temperature nonuniformity length scale. The usual gyrokinetic ordering is achieved for $\varepsilon_k \sim \varepsilon_\omega \sim \varepsilon_\delta \sim \varepsilon_{\nabla_{\mathrm{eq}}} \sim \varepsilon \sim 10^{-3}$ and $\varepsilon_\perp \sim 1$. For longer wavelengths such that $\varepsilon_\perp \ll 1$ we obtain the drift kinetic ordering.

C. ITG instability

The ITG instabilities correspond to small scale instabilities which start in the region where local temperature gradient exceeds local density gradient by some amount. Due to the existence of energy invariants in the system the perturbated modes can not grow unbounded and after a linear phase of exponential increase, a local quasilinear saturation takes place leading to flattening of the local temperature profile. In the nonlinear phase, the existence of broad wave spectrum involving mode coupling phenomena and nonlinear resonant wave-particle interaction leads to a state of developed plasma turbulence and to the appearance of anomalous heat transport.

Figures 3–5 illustrate some examples of initial radial profiles that we consider for ion density and temperature at equilibrium. In order to compare numerical results to analytical ones and thus to validate the code, we consider the case where in Eqs. (38) and (39) there is no polarization drift, i.e., the second-order differential operator in the transverse direc-

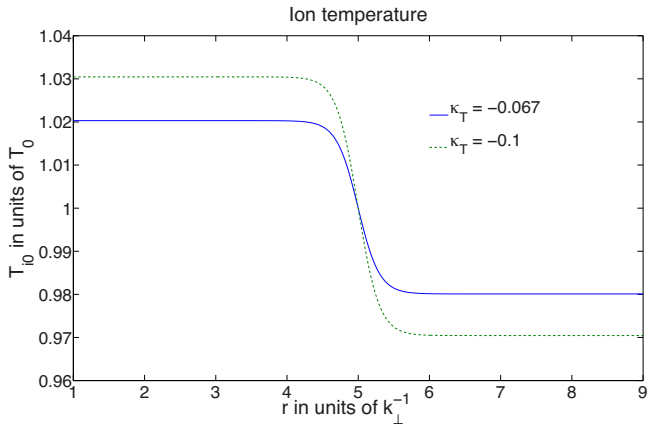

FIG. 4. (Color online) Initial ion temperature profile.

tion is removed ($\eta_2=0$). In that case a local (in the radial direction) linear analysis can be performed (see [32,47]), resulting in algebraic dispersion relation which can be rigorously solved and giving rise to analytical growth rate for the ITG instability. For this test case we take the dimensionless parameters such as $\varepsilon_\omega=\varepsilon_k=\varepsilon_\delta=10^{-3}$, the radial domain such as $r\in[1,5]$, and the perturbative toroidal-poloidal mode such as $(m,n)=(20,1)$. The results are summarized in Table I.

In spite of good agreement between numerical and theoretical linear growth rate values, the model (36)–(39) without polarization drift ($\eta_2=0$) is not well-posed and thus has no sense in a nonlinear regime because there is neither differential operator nor physical mechanism which prevent the excitation of small scale without damping. In other words, all the modes in the limit $k_\perp\to\infty$ are unstable which means that the solution blows up in a finite time.

Therefore, the next test case is to compare the linear growth rate of ITG instability given by the quasilinear model (36)–(39), referred to as QL, which is solved by a Runge-Kutta discontinuous Galerkin method and the full nonlinear model (7) and (8), referred to as NL, which is solved by a Runge-Kutta semi-Lagrangian method and has been developed in another paper [48]. For this test case we choose a radial domain such as $r\in[1,9]$ and $z,\theta\in[0,2\pi]$. The dimensionless parameters ε_ω, ε_k, and ε_δ are set to 10^{-3} and the

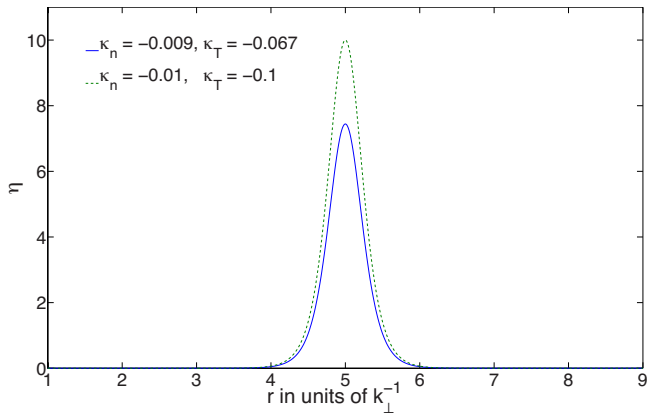

FIG. 5. (Color online) Initial η profile.

TABLE I. Comparison of analytical and numerical growth rate in the case of no polarization drift.

Case	$\kappa_n=1.5\times10^{-4}$	$\kappa_n=1.5\times10^{-4}$
	$\kappa_T=1.5\times10^{-3}$	$\kappa_T=1.5\times10^{-3}$
	$\mathcal{N}=8$	$\mathcal{N}=10$
	$v_{\max}=6$	$v_{\max}=5$
	$\tau=1$	$\tau=0.2$
γ_{theory}	0.80	1.80
γ_{numeric}	0.85	1.83
Case	$\kappa_n=1.5\times10^{-4}$	$\kappa_n=1.5\times10^{-4}$
	$\kappa_T=7.5\times10^{-4}$	$\kappa_T=6.45\times10^{-4}$
	$\mathcal{N}=10$	$\mathcal{N}=10$
	$v_{\max}=5$	$v_{\max}=5$
	$\tau=1$	$\tau=1$
γ_{theory}	0.22	0.097
γ_{numeric}	0.22	0.095

number of bags is $\mathcal{N}=6$. The results are summarized in Table II. From Table II we observe that the quasilinear model and the nonlinear model give the same ITG instability growth rate in the linear regime.

Let us now look at the nonlinear regime and saturation level of ITG instability. Figures 6 and 7 show the evolution of the logarithm of L^2-norm of the electrical potential at $r=r_0$ for the QL and NL models. On the other hand, Figs. 8 and 9 depict the corresponding mean heat flux

$$Q(t,r)=\sum_j \mathcal{A}_j\int\frac{d\theta}{2\pi}\frac{dz}{L_z}\left(\frac{v_j^{+3}}{3}-\frac{v_j^{-3}}{3}\right)(\mathbf{e}_z\times\nabla\phi)\cdot\mathbf{e}_r$$

at $r=r_0$. For the case (Figs. 6 and 8) where radial gradients are $\kappa_n=-0.009k_\perp^{-1}$ and $\kappa_T=-0.067k_\perp^{-1}$, the perturbative mode is $(m,n)=(10,3)$ and the discretization parameters are $\Delta t_{\text{QL}}=\Delta t_{\text{NL}}=4\times10^{-3}\omega^{-1}(\sim4\Omega_0^{-1})$, $\Delta r_{\text{QL}}=1.25\times10^{-1}k_\perp^{-1}$, $\Delta r_{\text{NL}}=6.25\times10^{-2}k_\perp^{-1}$, $\Delta z_{\text{QL}}=9.80\times10^{-3}k_\parallel^{-1}$, $\Delta z_{\text{NL}}=4.90$

TABLE II. Comparison of QL and NL growth rate.

Case	$\kappa_n=-0.02$	$\kappa_n=-0.03$	$\kappa_n=-0.04$
	$\kappa_T=-0.1625$	$\kappa_T=-0.24$	$\kappa_T=-0.32$
	$(m,n)=(6,3)$	$(m,n)=(6,3)$	$(m,n)=(6,3)$
γ_{QL}	1.70	2.12	2.44
γ_{NL}	1.70	2.12	2.44
Case	$\kappa_n=-0.02$	$\kappa_n=-0.01$	$\kappa_n=-0.01$
	$\kappa_T=-0.40$	$\kappa_T=-0.10$	$\kappa_T=-0.08$
	$(m,n)=(6,3)$	$(m,n)=(6,3)$	$(m,n)=(6,3)$
γ_{QL}	4.30	1.25	0.74
γ_{NL}	4.30	1.25	0.74
Case	$\kappa_n=-0.01$	$\kappa_n=-0.009$	$\kappa_n=-0.009$
	$\kappa_T=-0.075$	$\kappa_T=-0.069$	$\kappa_T=-0.067$
	$(m,n)=(6,3)$	$(m,n)=(10,3)$	$(m,n)=(10,3)$
γ_{QL}	0.56	0.65	0.568
γ_{NL}	0.56	0.65	0.568

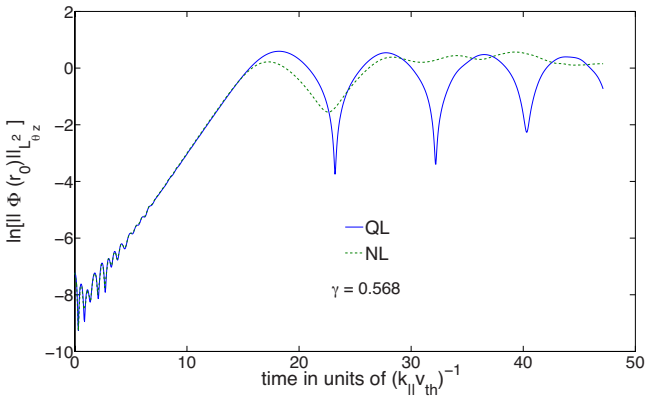

FIG. 6. (Color online) L^2-norm at $r=r_0$ of the electrical potential, $\kappa_n=-0.009$, $\kappa_T=-0.067$.

$\times 10^{-2}k_{\|}^{-1}$, $\Delta\theta_{\mathrm{NL}}=2.45\times10^{-2}$, $N_{r,\mathrm{QL}}=64$, $N_{r,\mathrm{NL}}=128$, $N_{z,\mathrm{QL}}=64$, $N_{z,\mathrm{NL}}=128$, and $N_{\theta,\mathrm{NL}}=256$. For the case (Figs. 7 and 9) where radial gradients are $\kappa_n=-0.01k_{\perp}^{-1}$ and $\kappa_T=-0.1k_{\perp}^{-1}$, the perturbative mode is $(m,n)=(6,3)$ and the discretization parameters are $\Delta t_{\mathrm{QL}}=4\times10^{-3}\omega^{-1}(\sim4\Omega_0^{-1})$, $\Delta t_{\mathrm{QL}}=7.85\times10^{-3}\omega^{-1}(\sim7.85\Omega_0^{-1})$ $\Delta r_{\mathrm{QL}}=1.25\times10^{-1}k_{\perp}^{-1}$, $\Delta r_{\mathrm{NL}}=6.25\times10^{-2}k_{\perp}^{-1}$, $\Delta z_{\mathrm{QL}}=\Delta z_{\mathrm{NL}}=9.80\times10^{-2}k_{\|}^{-1}$, $\Delta\theta_{\mathrm{NL}}=4.90\times10^{-2}$, $N_{r,\mathrm{QL}}=64$, $N_{r,\mathrm{NL}}=128$, $N_{z,\mathrm{QL}}=N_{z,\mathrm{NL}}=64$, and $N_{\theta,\mathrm{NL}}=128$. In every case $\tau=1$, $\varepsilon_\omega=\varepsilon_k=\varepsilon_\delta=10^{-3}$, $v_{\max}=5v_{thi}$, $r_{\min}=1k_{\perp}^{-1}\sim1\rho_i$, $r_{\max}=9k_{\perp}^{-1}\sim9\rho_i$, $z\in[0,2\pi k_{\perp}^{-1}]$, $\theta\in[0;2\pi]$, and $\mathcal{N}=6$.

Although in the linear regime QL and NL models give the same results, we observe that in the nonlinear regime their behavior slightly differs, as expected. We notice that the level of L^2-norm of electrical potential (Figs. 6 and 7) and mean heat flux (Figs. 8 and 9) are always a little greater for QL than NL. This remark can be explained by the fact that in the QL model most of the nonlinear couplings are removed and thus the saturation takes place with a time delay and an additional amount of electrical energy. Even if in the nonlinear regime QL and NL solutions are different, they remain qualitatively at the same level. Therefore, the QL model constitutes a relative good approximation of the NL model even in the nonlinear phase. As a result, the underlying idea of the quasilinear analysis, i.e., the diffusive nature of the radial transport [see the radial Fokker-Planck equation (27)], is also

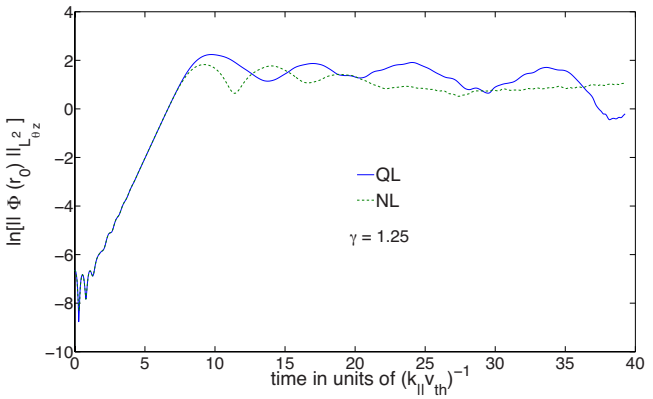

FIG. 7. (Color online) L^2-norm at $r=r_0$ of the electrical potential, $\kappa_n=-0.01$, $\kappa_T=-0.1$.

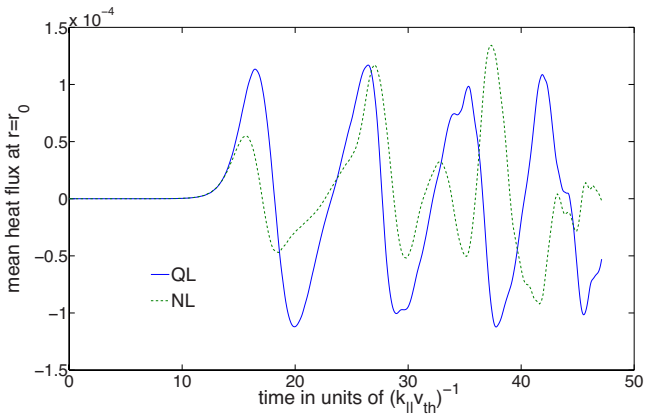

FIG. 8. (Color online) Normalized mean heat flux at $r=r_0$, $\kappa_n=-0.009$, $\kappa_T=-0.067$.

validated in the numerical simulation framework by the numerical approximation of the QL model, allowing us to obtain an estimate of the turbulent transport which is of the same order as the NL one.

Finally let us turn to the invariant conservation in both codes. It is well known that the Vlasov equation conserves many physical and mathematical quantities such that mass, kinetic entropy, total energy, every L^p-norm, and more generally any phase-space integral of $\beta(f)$ where β is a regular function. Obviously these conservation properties are retrieved with the gyro-water-bag model by using the distribution function (6) in the definition of the considered quantities, resulting in expressions involving integrals on the bags. We define the relative error $RE(\mathcal{Q})$ of the conserved quantity $\mathcal{Q}$ as $RE(\mathcal{Q})(t)=[\mathcal{Q}(t)-\mathcal{Q}(0)]/\mathcal{Q}(0)$. Therefore, Figs. 10 and 11 show the evolution of $RE(\|f\|_{L^1})$, Figs. 12 and 13 represent $RE(\|f\|_{L^2})$, and Figs. 14 and 15 depict the time evolution of $RE(\text{entropy of } f)$. For the QL code, in the case corresponding to $\kappa_n=-0.009$ and $\kappa_T=-0.067$ the relative error of the L^2-norm, L^1-norm (or mass), and kinetic entropy is less than 10^{-12} and for the case where the radial gradients are $\kappa_n=-0.01$ and $\kappa_T=-0.1$, their relative errors remain below 10^{-9}. We notice that these conservation are better than those obtained for the NL code in the nonlinear regime. These results can be explained by the fact that growing small scale

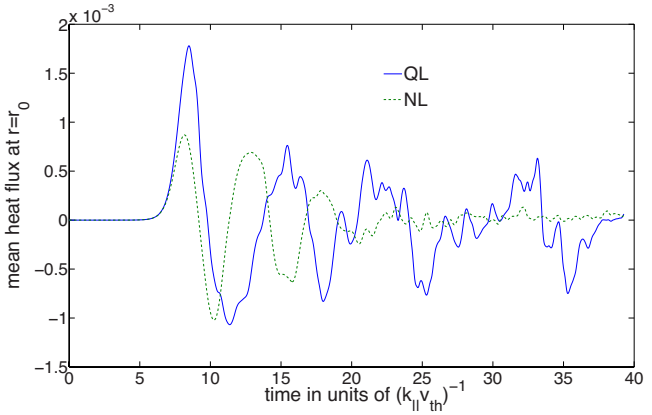

FIG. 9. (Color online) Normalized mean heat flux at $r=r_0$, $\kappa_n=-0.01$, $\kappa_T=-0.1$.

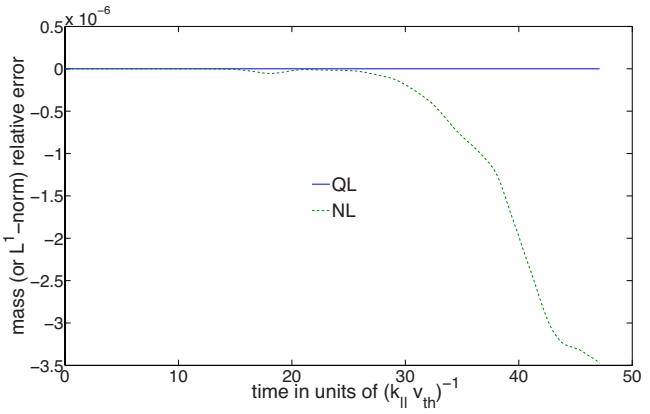

FIG. 10. (Color online) Relative error on the L^1-norm (or mass) of f, $\kappa_n=-0.009$, $\kappa_T=-0.067$.

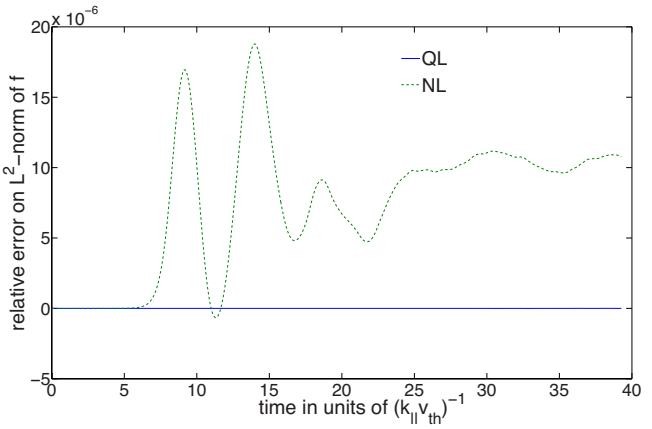

FIG. 13. (Color online) Relative error on the L^2-norm of f, $\kappa_n=-0.01$, $\kappa_T=-0.1$.

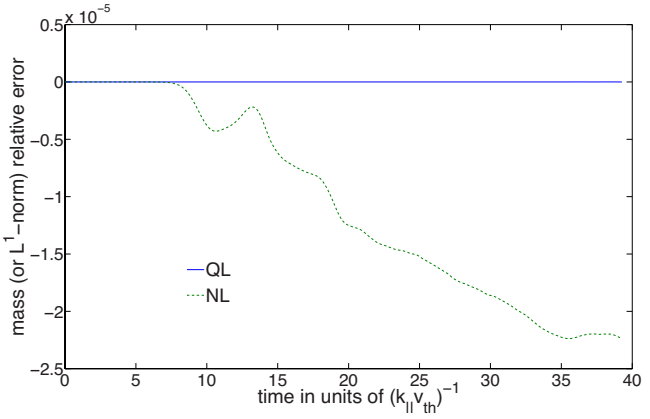

FIG. 11. (Color online) Relative error on the L^1-norm (or mass) of f, $\kappa_n=-0.01$, $\kappa_T=-0.1$.

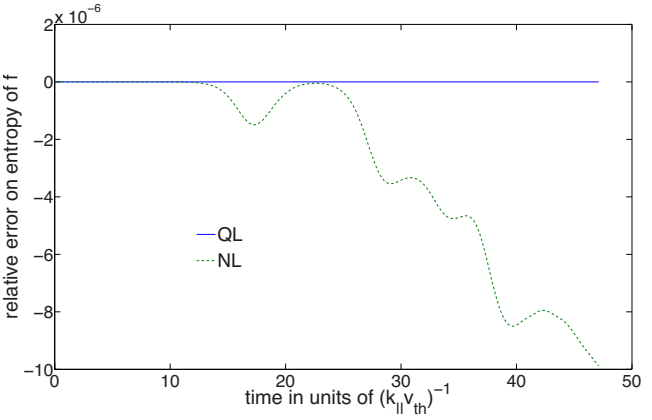

FIG. 14. (Color online) Relative error on the entropy of f, $\kappa_n=-0.009$, $\kappa_T=-0.067$.

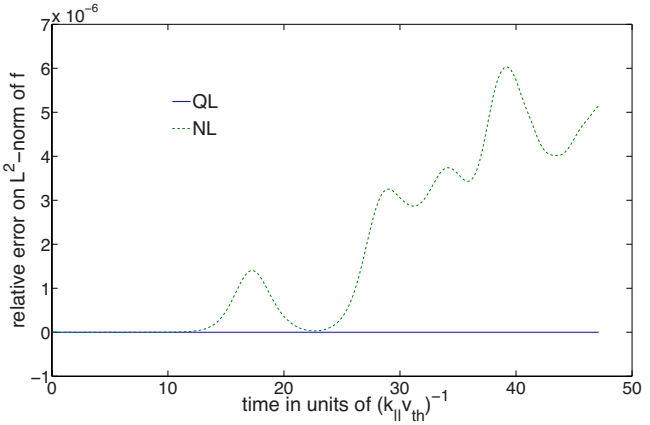

FIG. 12. (Color online) Relative error on the L^2-norm of f, $\kappa_n=-0.009$, $\kappa_T=-0.067$.

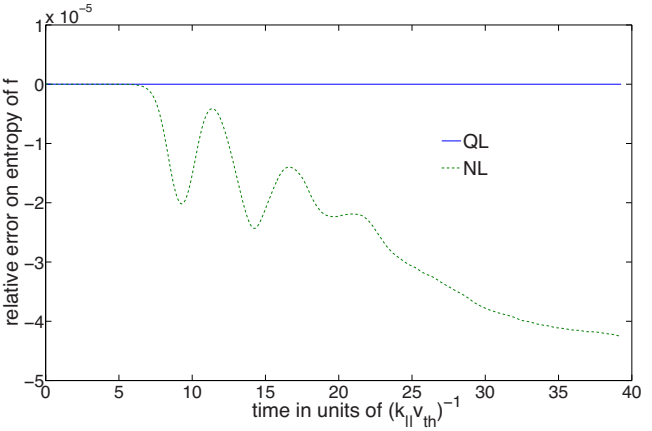

FIG. 15. (Color online) Relative error on the entropy of f, $\kappa_n=-0.01$, $\kappa_T=-0.1$.

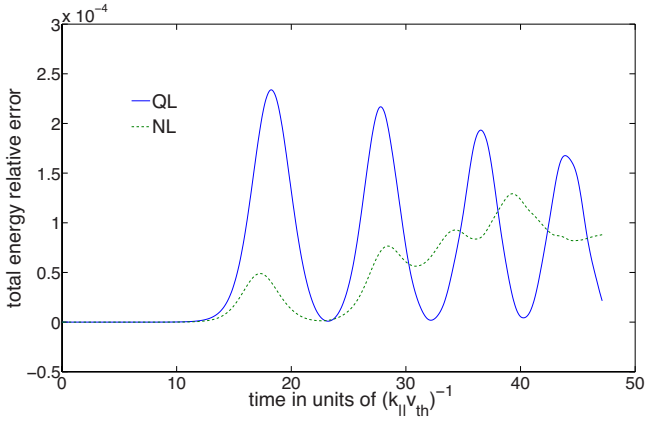

FIG. 16. (Color online) Relative error on the total energy, $\kappa_n = -0.009$, $\kappa_T = -0.067$.

poloidal structures whose size is smaller than the cell size are smoothed and then information is irreversibly lost resulting in deviations for every conserved quantity. Let us notice that in the NL code all poloidal modes, bounded by the mesh discretization in θ, can participate in the nonlinear regime whereas in the QL code they are fixed *a priori* (here to $m = 10$ or $m = 6$). Nevertheless even for the NL code the relative error always stays less than 10^{-4}.

The conservation of energy is most difficult to satisfy as in PIC codes [49] or Vlasov codes [10]. In term of energy conservation, the NL model behaves better than the QL one. In the light of the quasilinear analysis previously done, we know that the total energy is only conserved up to second order in the perturbation, thus it explains why energy conservation is less good in the case of the QL model. However, this conservation is still correct, even quite good, as the relative error always remains below 3×10^{-4} for $\kappa_n = -0.009/\kappa_T = -0.067$ and below 5×10^{-3} for $\kappa_n = -0.01/\kappa_T = -0.1$ (see Figs. 16 and 17).

VI. CONCLUSION

In this paper we have considered the water-bag weak solution of the Vlasov gyrokinetic equation, resulting in the development of the gyro-water-bag model. From this model we have shown the diffusive nature of the radial transport, through an analytical quasilinear analysis leading to Fokker-Planck equations for the bags in the radial direction. Nonlinear diffusion terms on the mean flow (zonal flow) appear as source terms of the Fokker-Planck equations which lead to a reaction-diffusion model. This is the back reaction of the turbulent diffusion which can lead to the formation of transport barriers. This reaction-diffusion model has been checked by numerical simulations through the derivation of a self-consistent quasilinear code, suitable for a numerical simulation framework, and making use of a Runge-Kutta discontinuous Galerkin scheme. In order to validate the quasilinear approach we have performed various comparisons with a full nonlinear gyro-water-bag code [48]. As a result, the quasilinear approach proves to be a good approximation of the full nonlinear one since the quasilinear estimate of the turbulent transport is of the same order of the nonlinear one. Further developments using reaction-diffusion-water-bag model (pertinent to magnetic confinement purpose) are now under consideration. Although comparisons between gyro-water-bag code and gyrokinetic code is beyond the scope of the present paper, it should be done and it will be the starting point of further studies.

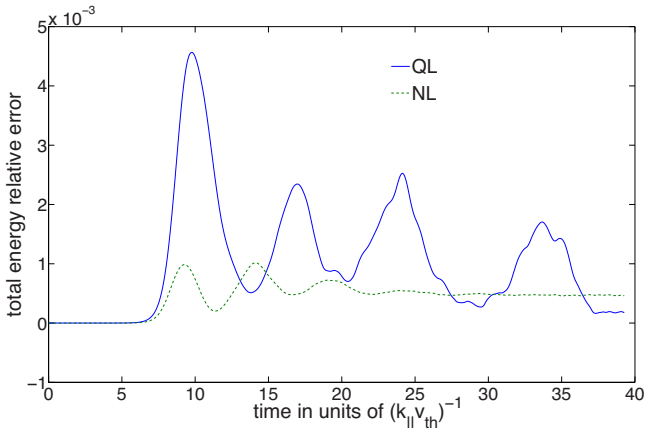

FIG. 17. (Color online) Relative error on the total energy, $\kappa_n = -0.01$, $\kappa_T = -0.1$.

APPENDIX A: DISCONTINUOUS GALERKIN DISCRETIZATION OF THE GYRO-WATER-BAG MODEL

Let us first set

$$\mathcal{P}_h(\Omega) = \{ \psi \mid \psi_{|K} \in \mathcal{P}(K), \forall K \in \mathcal{M}_h \},$$

where $\mathcal{P}(K)$ is a space of polynomials of any degree on the finite element K. Therefore, to determine the approximate solution $(v^{\pm}_{h,j0}, \mathrm{Re}\, V^{\pm}_{h,jm}, \mathrm{Im}\, V^{\pm}_{h,jm}, \phi_{h,0}, \mathrm{Re}\, \Phi_{h,m}, \mathrm{Im}\, \Phi_{h,m})_{|K} \in \otimes^6 \mathcal{P}(K)$ for $t > 0$, using the variational formulations (40)–(45), on each element K of $\mathcal{M}_h$ we impose that, for all $\varphi_h \in \mathcal{P}(K)$, for all $j = 1, \ldots, \mathcal{N}$, for $\alpha \in \{1, 2\}$,

$$\begin{aligned}
&\partial_t \int_K dK v^{\pm}_{h,j0} \varphi_h - \frac{1}{2} \int_K dK (v^{\pm}_{h,j0})^2 \partial_z \varphi_h + \int_{\partial K} d\Gamma \langle f n_{K,z} \rangle (v^{\pm}_{h,j0}) \\
&\quad \times \varphi_h + Z_i \varepsilon_\delta \int_K dK \varphi_h E_{h,0z} - \eta_1 \sum_{m>0} m \left[\int_K dK V^{\pm}_{h,jm} \right. \\
&\quad \times \Phi_{h,m} \partial_r \left(\frac{\varphi_h}{2r} \right) - \left. \int_{\partial K} d\Gamma \langle V^{\pm}_{h,jm} \times \Phi_{h,m} n_{K,r} \rangle \frac{\varphi_h}{2r} \right] \\
&\quad - \sum_{m>0} \left(\frac{1}{4} \int_K dK |V^{\pm}_{h,jm}|^2 \partial_z \varphi_h - \frac{1}{2} \int_{\partial K} d\Gamma [\langle f n_{K,z} \rangle (\mathrm{Re}\, V^{\pm}_{h,jm}) \right. \\
&\quad \left. + \langle f n_{K,z} \rangle (\mathrm{Im}\, V^{\pm}_{h,jm})] \varphi_h \right) = 0 \qquad \text{(A1)}
\end{aligned}$$

with

$$\int_K dK\varphi_h E_{h,0z} = -\int_K dK\phi_{h,0}\partial_z\varphi_h + \int_{\partial K} d\Gamma\langle\phi_{h,0}n_{K,z}\rangle\varphi_h \tag{A2}$$

and

$$\partial_t\int_K dKV_{h,jm}^{\pm\alpha}\varphi_h - \int_K dKv_{h,j0}^{\pm}V_{h,jm}^{\pm\alpha}\partial_z\varphi_h + \eta_1\int_K dK\frac{\gamma_\alpha m}{r}(E_{h,0r}V_{h,jm}^{\pm\beta} - \partial_r v_{h,j0}^{\pm}\Phi_{h,m}^{\beta})\varphi_h + \int_{\partial K} d\Gamma\langle v_{h,j0}^{\pm}V_{h,jm}^{\pm\alpha}n_{K,z}\rangle\varphi_h + Z_i\varepsilon_\delta\int_K dKE_{h,mz}^{\alpha}\varphi_h = 0, \tag{A3}$$

where

$$\int_K dK\varphi_h E_{h,0r} = -\int_K dK\phi_{h,0}\partial_r\varphi_h + \int_{\partial K} d\Gamma\langle\phi_{h,0}n_{K,r}\rangle\varphi, \tag{A4}$$

$$\int_K dK\partial_r v_{h,j0}^{\pm}\varphi_h = -\int_K dKv_{h,j0}^{\pm}\partial_r\varphi_h + \int_{\partial K} d\Gamma\langle v_{h,j0}^{\pm}n_{K,r}\rangle\varphi_h, \tag{A5}$$

$$\int_K dK\varphi_h E_{h,mz}^{\alpha} = -\int_K dK\Phi_{h,m}^{\alpha}\partial_z\varphi_h + \int_{\partial K} d\Gamma\langle\Phi_{h,m}^{\alpha}n_{K,z}\rangle\varphi_h. \tag{A6}$$

In Eqs. (A1)–(A6) we have replaced the flux terms at the boundary of the cell K, by numerical fluxes (bracket notation) because the terms arising from the boundary of the cell K are not well defined or have no sense since all unknowns are discontinuous (by construction of the space of approximation) on the boundary ∂K of the element K. Now it remains to define these numerical fluxes. For two adjacent cells K^ℓ and K^{r} (r denotes the right cell and ℓ the left one) of $\mathcal{M}_h$ and a point P of their common boundary at which the vector n_{K^σ}, $\sigma\in\{\mathrm{r},\ell\}$ are defined, we set $\varphi_h^\sigma(P) = \lim_{\varepsilon\to 0}\varphi_h(P-\varepsilon n_{K^\sigma})$ and call these values the traces of φ_h from the interior of K^σ. Therefore, the numerical flux at P is a function of the left and right traces of the unknowns considered. For example,

$$\langle fn_{K^\ell,z}\rangle(v_{h,j0}^{\pm})(P) = \langle fn_{K^\ell,z}\rangle[v_{h,j0}^{\pm,\ell}(P), v_{h,j0}^{\pm,\mathrm{r}}(P)].$$

Besides the numerical flux must be consistent with the nonlinearity $fn_{K^\ell,z}$, which means that we should have $\langle fn_{K^\ell,z}\rangle(v,v) = f(v)n_{K^\ell,z}$. In order to give monotone scheme in case of piecewise-constant approximation the numerical flux must be conservative, i.e.,

$$\langle fn_{K^\ell,z}\rangle[v_{h,j0}^{\pm,\ell}(P), v_{h,j0}^{\pm,\mathrm{r}}(P)] + \langle fn_{K^{\mathrm{r}},z}\rangle[v_{h,j0}^{\pm,\mathrm{r}}(P), v_{h,j0}^{\pm,\ell}(P)] = 0 \tag{A7}$$

and the mapping $v\mapsto\langle fn_{K^\ell,z}\rangle(v,\cdot)$ must be nondecreasing. There exists several examples of numerical fluxes satisfying the above requirements: The Godunov flux, the Engquist-Osher flux, the Lax-Friedrichs flux (see [45]). For the numerical fluxes $\langle V_{h,jm}^{\pm}\times\Phi_{h,m}n_{K,r}\rangle$, $\langle fn_{K,z}\rangle(\mathrm{Re}\ V_{h,jm}^{\pm})$, and $\langle fn_{K,z}\rangle(\mathrm{Im}\ V_{h,jm}^{\pm})$ we choose the average flux. For fluxes $\langle\phi_{h,0}n_{K,z}\rangle$, $\langle\phi_{h,0}n_{K,r}\rangle$, $\langle v_{h,j0}^{\pm}n_{K,r}\rangle$, and $\langle\Phi_{h,m}^{\alpha}n_{K,z}\rangle$ we can choose the average, left-hand or right-hand flux. Finally for the numerical flux $\langle v_{h,j0}^{\pm}V_{h,jm}^{\pm\alpha}n_{K,z}\rangle$ we can choose two different upwind fluxes

$$\langle v_{h,j0}^{\pm}V_{h,jm}^{\pm\alpha}n_{K,z}\rangle = \langle v_{h,j0}^{\pm}n_{K,z}\rangle^{\Delta}V_{h,jm}^{\pm\alpha,\ell} + \langle v_{h,j0}^{\pm}n_{K,z}\rangle^{\nabla}V_{h,jm}^{\pm\alpha,\mathrm{r}},$$

where

$$\langle v_{h,j0}^{\pm}n_{K,z}\rangle^{\Delta} = (v_{h,j0}^{\pm,\ell})^{\Delta}|n_{K,z}|,$$

$$\langle v_{h,j0}^{\pm}n_{K,z}\rangle^{\nabla} = (v_{h,j0}^{\pm,\mathrm{r}})^{\nabla}|n_{K,z}|$$

or

$$\langle v_{h,j0}^{\pm}n_{K,z}\rangle = |n_{K,z}|[(1-\eta)v_{h,j0}^{\pm,\ell} + \eta v_{h,j0}^{\pm,\mathrm{r}}],$$

where $\eta\in[0,1]$ and with the notation $z^{\Delta}=\max(z,0)$ and $z^{\nabla}=\min(z,0)$.

APPENDIX B: RUNGE-KUTTA INTEGRATION SCHEME

For numerical stability considerations we must choose $k+1$ stage Runge-Kutta method of order $k+1$ for DG discretization using polynomials of degree k if we do not want our CFL number to be too small. As we take polynomial of degree 2 we choose the third-order strong stability-preserving Runge-Kutta method [46]:

$$X_h(t_1) = X_h(t^n) + \Delta tL_{h,X_h}[v_{h,j0}^{\pm}(t^n), V_{h,jm}^{\pm}(t^n), \phi_{h,0}(t^n), \Phi_{h,m}(t^n)],$$

$$X_h(t_2) = \tfrac{3}{4}X_h(t^n) + \tfrac{1}{4}X_h(t_1) + \tfrac{1}{4}\Delta tL_{h,X_h}[v_{h,j0}^{\pm}(t_1), V_{h,jm}^{\pm}(t_1), \phi_{h,0,}(t_1), \Phi_{h,m}(t_1)],$$

$$X_h(t^{n+1}) = \tfrac{1}{3}X_h(t^n) + \tfrac{2}{3}X_h(t_2) + \tfrac{2}{3}\Delta tL_{h,X_h}[v_{h,j0}^{\pm}(t_2), V_{h,jm}^{\pm}(t_2), \phi_{h,0,}(t_2), \Phi_{h,m}(t_2)],$$

$\forall X_h\in\Lambda$ with $t^n=n\Delta T$, $\Delta t=T/N_T$, and t_1 and t_2 time between t^n and t^{n+1}. For the discretization of the initial condition we take $[v_{h,j0}^{\pm}(t=0), V_{h,jm}^{\pm}(t=0)]$ on the cell K to be the L^2 projection of $[v_{j0}^{\pm}(t=0), V_{jm}^{\pm}(t=0)]$ on $\otimes^3\mathcal{P}(K)$.

APPENDIX C: DISCONTINUOUS GALERKIN DISCRETIZATION OF THE QUASINEUTRALITY EQUATION

Using Green formula we can rewrite the problems (47)–(51) in a variational form suitable for its numerical approximation which consists in finding $\sigma_h\in\mathcal{P}_h(\Omega)$ and $\phi_h\in\mathcal{P}_h(\Omega)$ such that for all $\varphi_h,\psi_h\in\mathcal{P}_h(\Omega)$, for all $K\in\mathcal{M}_h$,

$$\int_K \varrho^{-1}\sigma_h\varphi_h dK = \int_K \phi_h\partial_r\varphi_h dK - \int_{\partial K}\hat{\phi}_K\varphi_h n_{K^\ell,r}d\Gamma, \tag{C1}$$

$$\int_K \sigma_h \partial_r \psi_h dK = \int_{\partial K} \hat{\sigma}_K n_{K^\ell,r} \psi_h d\Gamma + \int_K \chi \phi_h \psi_h dK - \int_K \rho_h \psi_h dK, \tag{C2}$$

where σ_h and ϕ_h are approximations to $\sigma=-\varrho\partial_r\phi$ and ϕ, respectively, and ρ_h stands for the approximation of ρ in $\mathcal{P}_h(\Omega)$. The numerical fluxes $\hat{\sigma}_K$ and $\hat{\phi}_K$ are approximations to $\sigma=-\varrho\partial_r\phi$ and to ϕ, respectively, on the boundary of the cell K. If we set n the outward unit normal to $\partial\Omega$, $\mathcal{E}_h^\circ$ the set of interior edges of $\mathcal{M}_h$, $\mathcal{E}_h^\partial$ the set of boundary edges of $\mathcal{M}_h$ and if we use the notations $[\![\varphi_h]\!]=\varphi_h^r n_{K^\ell,r}+\varphi_h^\ell n_{K^r,r}$ and $\{\varphi_h\}=\frac{1}{2}(\varphi_h^r+\varphi_h^\ell)$, then for $\varphi,\psi\in\Pi_{K\in\mathcal{M}_h}L^2(\partial K)$ we have

$$\sum_{K\in\mathcal{M}_h}\int_{\partial K}\psi_{K^\ell}\varphi_{K^\ell}n_{K^\ell,r}d\Gamma = \int_{\mathcal{E}_h^\circ}([\![\psi]\!]\{\varphi\}+[\![\varphi]\!]\{\psi\})d\Gamma + \int_{\mathcal{E}_h^\partial}\psi\varphi n_r d\Gamma. \tag{C3}$$

If we take $\varphi_h=\sigma_h$ in (C1), $\psi_h=\phi_h$ in (C2), summing over the cell K and using (C3) we obtain

$$\mathcal{R}_h + \int_\Omega \varrho^{-1}|\sigma_h|^2 dK + \int_\Omega \chi|\phi_h|^2 dK = \int_\Omega \rho_h\phi_h dK, \tag{C4}$$

where

$$\mathcal{R}_h = \int_{\mathcal{E}_h^\circ}(\{\hat{\sigma}_h-\sigma_h\}[\![\phi_h]\!]+\{\hat{\phi}_h-\phi_h\}[\![\sigma_h]\!])d\Gamma + \int_{\mathcal{E}_h^\partial}(\phi_h(\hat{\sigma}_h-\sigma_h)+\hat{\phi}_h\sigma_h)n_r d\Gamma. \tag{C5}$$

Let us now choose the numerical fluxes as follows:

$$\hat{\sigma}_h = \{\sigma_h\}+\alpha_{11}[\![\phi_h]\!]+\alpha_{12}[\![\sigma_h]\!] \quad \text{on } \mathcal{E}_h^\circ, \tag{C6}$$

$$\hat{\phi}_h = \{\phi_h\}-\alpha_{11}[\![\phi_h]\!]+\alpha_{22}[\![\sigma_h]\!] \quad \text{on } \mathcal{E}_h^\circ, \tag{C7}$$

$$\hat{\sigma}_h = \sigma_h^\ell+\alpha_{11}\phi_h^\ell n_r, \quad \hat{\phi}_h=0 \quad \text{on } \mathcal{E}_h^\partial\cap\Gamma_D, \tag{C8}$$

$$\hat{\sigma}_h = 0, \quad \hat{\phi}_h=\phi_h^\ell+\alpha_{22}\sigma_h^\ell n_r \quad \text{on } \mathcal{E}_h^\partial\cap\Gamma_N, \tag{C9}$$

where $\alpha_{11}>0$, $\alpha_{22}\geq 0$, $\alpha_{12}\in\mathbb{R}$, and Γ_D (respectively, Γ_N) denotes the boundary edges subset of $\mathcal{E}_h^\partial$ where Dirichlet conditions (respectively, Neumann) are applied. If we plug (C6)–(C9) into (C5) then we obtain

$$\mathcal{R}_h = \int_{\mathcal{E}_h^\circ}(\alpha_{11}[\![\phi_h]\!]^2+\alpha_{22}[\![\sigma_h]\!]^2)d\Gamma + \int_{\mathcal{E}_h^\partial\cap\Gamma_D}\alpha_{11}|\phi_h|^2 d\Gamma + \int_{\mathcal{E}_h^\partial\cap\Gamma_N}\alpha_{22}|\sigma_h|^2 d\Gamma \geq 0.$$

If we set $\rho_h=0$ in (C4) then we obtain $[\![\phi_h]\!]_{\mathcal{E}_h^\circ}=0$, $\phi_{h_{|\Gamma_D}}=0$, $\sigma_h=0$, and $\phi_h=0$ since ϱ, χ, $\alpha_{11}>0$, and $\alpha_{22}\geq 0$. Therefore, $\phi_h=0$ on $\bar{\Omega}$ and the approximate solution ϕ_h is well defined. Now that the method supplies a unique approximate solution, let us compute it. If we take Eq. (C1), sum over the cell K, by using (C3) we obtain

$$a(\sigma_h,\varphi_h)-b(\phi_h,\varphi_h)=0, \quad \forall\ \varphi_h\in\mathcal{P}_h(\Omega), \tag{C10}$$

where the bilinear forms $a(\cdot,\cdot)$ and $b(\cdot,\cdot)$ are

$$a(u,v) = \int_\Omega \varrho^{-1}uv dK + \alpha_{22}\left(\int_{\mathcal{E}_h^\circ}[\![u]\!][\![v]\!]d\Gamma + \int_{\mathcal{E}_h^\partial\cap\Gamma_N}(un_r)(vn_r)\right),$$

$$b(w,u) = \int_\Omega \partial_r uw dK + \int_{\mathcal{E}_h^\circ}[\![u]\!](\alpha_{12}[\![w]\!]-\{w\})d\Gamma - \int_{\mathcal{E}_h^\partial\cap\Gamma_N} un_r w.$$

Using integration by part we obtain

$$-\int_K \sigma_h\partial_r\varphi_h dK = -\int_{\partial K}\sigma_h n_{K^\ell,r}\varphi_h d\Gamma + \int_K \partial_r\sigma_h\varphi_h dK. \tag{C11}$$

If we add (C2) to (C11), sum over all cell K, and use (C3) then we obtain

$$b(\psi_h,\sigma_h)+c(\psi_h,\phi_h)=F(\psi_h), \quad \forall\ \psi_h\in\mathcal{P}_h(\Omega), \tag{C12}$$

where the bilinear form $c(\cdot,\cdot)$ and the linear form $F(\cdot)$ are, respectively,

$$c(w,p) = \alpha_{11}\int_{\mathcal{E}_h^\circ}[\![w]\!][\![p]\!]d\Gamma + \alpha_{11}\int_{\mathcal{E}_h^\partial} pw d\Gamma + \int_\Omega \chi pw dK$$

and

$$F(w) = \int_\Omega w\rho_h dK.$$

The variational formulation (C10) and (C12) leads to the matrix formulation, $\forall(\Psi_h,\Xi_h)$,

$$\Xi_h^T\mathcal{A}\Sigma_h-\Phi_h^T\mathcal{B}\Psi_h=0, \quad \Psi_h^T\mathcal{B}\Sigma_h-\Psi_h^T\mathcal{C}\Phi_h=\Psi_h^T F_h,$$

which is equivalent to solving the linear system

$$\Sigma_h=\mathcal{A}^{-1}\mathcal{B}^T\Phi_h, \quad (\mathcal{B}\mathcal{A}^{-1}\mathcal{B}^T+\mathcal{C})\Phi_h=F_h. \tag{C13}$$

We can solve (C13) by direct (LU decomposition, for example) or iterative methods (conjugate gradient, for example) of linear algebra. Let us note that if $\alpha_{22}=0$, then the matrix $\mathcal{A}$ is diagonal by block, and therefore it is easier to invert. Up to this point we have assumed that all integrals involved in the definition of the numerical schemes are

evaluated analytically. In fact all integrals can be reduced to the computation

$$\int_{-1}^{1} f(\xi)d\xi. \tag{C14}$$

To evaluate (C14) we use numerical integration or quadrature rules whose concept is the approximation of the integral by finite summation of the form

$$\int_{-1}^{1} f(\xi)d\xi \approx \sum_{i=0}^{Q-1} \omega_i f(\xi_i),$$

where ω_i are specified constants or weights and ξ_i represent abscissae of Q distinct points in the interval $-1 \leq \xi_i \leq 1$. There are many types of numerical integrations [50], here we choose Gaussian quadrature rules. In order to keep high-order accuracy, the quadrature rules should be exacted for polynomials of degree $2k+1$ on ∂K and $2k$ on K, where k is the degree of polynomial approximation [45].

[1] R. E. Waltz, Phys. Fluids **31**, 1962 (1988).
[2] H. Nordman, J. Weiland, and A. Jarmén, Nucl. Fusion **30**, 983 (1990).
[3] W. Dorland and G. W. Hammett, Phys. Fluids B **5**, 812 (1993).
[4] X. Garbet and R. E. Waltz, Phys. Plasmas **3**, 1898 (1996).
[5] G. Manfredi and M. Ottaviani, Phys. Rev. Lett. **79**, 4190 (1997).
[6] S. E. Parker, W. W. Lee, and R. A. Santoro, Phys. Rev. Lett. **71**, 2042 (1993).
[7] R. D. Sydora, V. K. Decyk, and J. M. Dawson, Plasma Phys. Controlled Fusion **38**, A281 (1996).
[8] Z. Lin, T. S. Hahm, W. W. Lee, W. M. Tang, and R. B. White, Phys. Plasmas **7**, 1857 (2000).
[9] G. Depret, X. Garbet, P. Bertrand, and A. Ghizzo, Plasma Phys. Controlled Fusion **42**, 949 (2000).
[10] V. Grandgirard *et al.*, J. Comput. Phys. **217**, 395 (2006).
[11] W. Dorland, F. Jenko, M. Kotschenreuther, and B. N. Rogers, Phys. Rev. Lett. **85**, 5579 (2000).
[12] J. Candy and R. E. Waltz, J. Comput. Phys. **186**, 545 (2003).
[13] Y. Sarazin, V. Grandgirard, E. Fleurence, X. Garbet, Ph. Ghendrih, P. Bertrand, and G. Depret, Plasma Phys. Controlled Fusion **47**, 1817 (2005).
[14] D. C. DePackh, J. Electron. Control **13**, 417 (1962).
[15] M. R. Feix, F. Hohl, and L. D. Staton, *Nonlinear Effects in Plasmas*, edited by G. Kalman and M. R. Feix (Gordon and Breach, New York, 1969), pp. 3–21.
[16] P. Bertrand and M. R. Feix, Phys. Lett. **28A**, 68 (1968).
[17] P. Bertrand and M. R. Feix, Phys. Lett. **29A**, 489 (1969).
[18] H. L. Berk and K. V. Roberts, in *Methods in Computational Physics* (Academic, New York, 1970), Vol. 9.
[19] U. Finzi, Plasma Phys. **14**, 327 (1972).
[20] M. Navet and P. Bertrand, Phys. Lett. **34A**, 117 (1971).
[21] P. Bertrand, Ph.D. thesis, Université de Nancy, 1972.
[22] P. Bertrand, J. P. Doremus, G. Baumann, and M. R. Feix, Phys. Fluids **15**, 1275 (1972).
[23] P. Bertrand, M. Gros, and G. Baumann, Phys. Fluids **19**, 1183 (1976).
[24] E. A. Frieman and L. Chen, Phys. Fluids **25**, 502 (1982).
[25] D. H. E. Dubin, J. A. Krommes, C. Oberman, and W. W. Lee, Phys. Fluids **26**, 3524 (1983).
[26] T. S. Hahm, Phys. Fluids **31**, 2670 (1988).
[27] A. J. Brizard and T. S. Hahm, Rev. Mod. Phys. **79**, 421 (2007).
[28] A. J. Brizard, Phys. Rev. Lett. **84**, 5768 (2000).
[29] F. R. Hansen, G. Knorr, J. P. Lynov, H. L. Pécseli, and J. J. Rasmussen, Plasma Phys. Controlled Fusion **31**, 173 (1989).
[30] G. Knorr and H. L. Pécseli, J. Plasma Phys. **41**, 157 (1989).
[31] W. W. Lee, Phys. Fluids **26**, 556 (1983).
[32] P. Morel *et al.*, Phys. Plasmas **14**, 112109 (2007).
[33] M. R. Feix, P. Bertrand, and A. Ghizzo, in *Advances in Kinetic Theory and Computing*, Series on Advances in Mathematics and Applied Science, edited by B. Perthame (World Scientific, Singapore, 1994), Vol. 22, pp. 42–82.
[34] N. G. Van Kampen, Physica **21**, 949 (1955).
[35] K. M. Case, Ann. Phys. **7**, 349 (1959).
[36] R. Z. Sagdeev and A. Galeev, *Nonlinear Plasma Theory* (Benjamin, New York, 1969).
[37] A. A. Vedenov, A. V. Gordeev, and L. I. Rudakov, Plasma Phys. **9**, 719 (1967).
[38] W. E. Drummond and P. Pines, Nucl. Fusion Suppl. **3**, 1049 (1962).
[39] A. N. Kaufman, J. Plasma Phys. **8**, 1 (1972).
[40] R. C. Davidson, *Methods in Nonlinear Plasma Theory* (Academic, New York, 1972).
[41] T. H. Dupree, Phys. Fluids **9**, 1773 (1966).
[42] Y. Idomura, M. Wakatani, and S. Tokuda, Phys. Plasmas **7**, 3551 (2000).
[43] P. H. Diamond, S.-I. Itoh, K. Itoh, and T. S. Hahm, Plasma Phys. Controlled Fusion **47**, R35 (2005).
[44] E. F. Keller and L. A. Segel, J. Theor. Biol. **26**, 399 (1970).
[45] B. Cockburn and C.-W. Shu, J. Sci. Comput. **16**, 173 (2001).
[46] S. Gottlieb, C.-W. Shu, and E. Tadmor, SIAM Rev. **43**, 89 (2001).
[47] P. Morel, E. Gravier, N. Besse, and P. Bertrand, Commun. Nonlinear Sci. Numer. Simul. **13**, 11 (2008).
[48] N. Besse and P. Bertrand (unpublished).
[49] Y. Idomura, S. Tokuda, and Y. Kishimoto, Nucl. Fusion **43**, 234 (2003).
[50] G. E. Karniadakis and S. J. Sherwin, *Spectral/hp Element Methods for Computational Fluid Dynamics* (Oxford University Press, Oxford, 1999).